MESOSCOPIC MODEL OF MICROSTRUCTURE EVOLUTION IN SHAPE MEMORY ALLOYS WITH APPLICATIONS TO NiMnGa

By

Martin Kružík

and

Tomáš Roubíček

IMA Preprint Series # 2003

(November 2004)

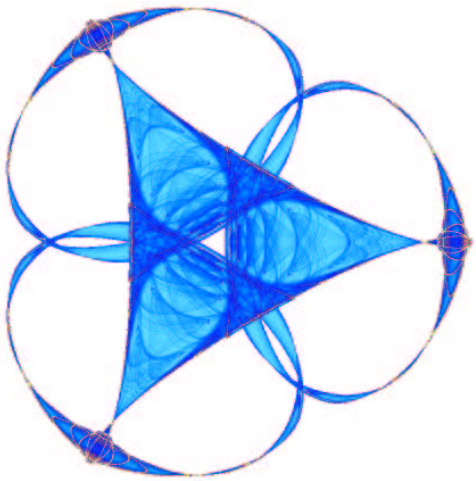

INSTITUTE FOR MATHEMATICS AND ITS APPLICATIONS

UNIVERSITY OF MINNESOTA
514 Vincent Hall
206 Church Street S.E.
Minneapolis, Minnesota 55455–0436

Phone: 612/624-6066 Fax: 612/626-7370
URL: http://www.ima.umn.edu

Mesoscopic model of microstructure evolution in shape memory alloys with applications to NiMnGa[1]

Martin Kružík* & Tomáš Roubíček**,*

*Institute of Information Theory and Automation, Academy of Sciences of the Czech Republic, Pod vodárenskou věží 4, CZ-182 08 Praha 8, Czech Republic
**Mathematical Institute, Charles University, Sokolovská 83, CZ-186 75 Praha 8

Abstract. This contribution presents a mesoscopic model of evolution of microstructure in alloys exhibiting shape-memory effects. Main features are a multi-well stored energy at large strains and rate-independent dissipation potential acting on volume fractions involved in the mesoscopic description of microstructure by Young measures. The focus is on analysis of an approximation scheme as well as on numerical simulations of single-crystal experiments with specific alloys.

Contents

[1]This is an extended preprint version of the paper "Mesoscopic model of microstructure evolution in shape memory alloys, its numerical analysis and computer implementation" submitted to the *Proceedings of the 3rd GAMM Seminar on microstructures.* (Ed C. Miehe), J Wiley.

1 Introduction, shape-memory alloys

Shape-memory alloys (=SMAs), as so-called smart materials, have enjoyed recently important applications especially in human medicine (e.g. vascular or dental implants) and mechanical or aerospace engineering, and have therefore been subjected to intensive theoretical and experimental research. SMAs exhibit specific *hysteretic* stress/strain/temperature response, which is called a *shape-memory effect* (=SME); cf. Figures 1b, 2 and 4 in this paper. The mechanism behind SME is quite simple: atoms tend to be arranged in different crystalographical configuration (in particular, having different symmetry groups) under different temperatures. At higher temperatures, atoms tend to form a grid with higher symmetry (typically cubic) which is referred to as the *austenite* phase while, at lower temperatures, they tend to form a lower-symmetrical grid (typically tetragonal, orthorhombic, monoclinic, or triclinic) called *martensite* phase. Due to symmetry, the lower-symmetrical grid may occur in several *variants* which can be combined (we speak about a coherent co-existence) with each other, forming thus so-called *twins* of two variants. Such a regular twined structure is called a laminate. Laminates can be combined in layers-within-layers to second-order (or even higher-order) laminates, or some other self-organization as wedges or branching can be observed and explained by mere crystallographic arguments, cf. [5, 6, 8, 21, 36, 39, 41]. These basic studies address primarily stress-free configurations. In general configurations exposed to outer loading, one has to consider the *free energy* which expresses a phenomenology of an energy, dependent on temperature, stored in interatomic links and atomic vibrations under a given deformation gradient and temperature. When loaded even more, the martensitic phase(variant)s can usually transform to each other (resp. also to a higher-symmetrical austenite), which is called re-orientation of martensite (resp. *martensitic phase transformation*). Depending whether only particular variants of martensite(s) or also a parent austenite is involved (i.e. depending on temperature), the resulted response is called *quasi-plasticity* and *pseudo-elasticity*, respectively. This is even a less understood phenomenon playing, however, equally important role in evolution of the microstructure. The phenomenology related to it describes a *dissipation* of the mechanical energy into heat or, to a smaller extent, acoustic emission.

Mathematical and computational modelling of SMAs represents a certain tool of theoretical understanding of transformation processes and may both complete experimental results and predict response of new materials or applications in engineering workpieces even before casted or built. The real situation in SMAs is essentially *multi-scale* which already creates variety of possibilities for modeling. Here we focus on a *mesoscopic* model playing, beside an "averaged" deformation and deformation gradients of particular phases (or phase variants), with volume fractions. This seems to be a successful compromise that allow us to describe scales of large single crystals as often used in labs, or even representative sample volumes of polycrystals. Besides, various dissipation mechanisms can be considered. Here we focus on a phenomenological degree-1 homogeneous potential which is related with a hysteretic response and with the fact that the phase transformations in

SMA are activated processes which are, if enough slow and isothermal, *rate independent*. For a certain survey of a wide menagerie of SMA models we refer to [47].

In Sections 2-3, we present a mesoscopic model proposed, after a preliminary scalar study [46], in [30]. The purpose of this paper is primarily to develop a certain approximation theory for this model, done in Section 4. After describing an implementation in Section 5, numerical simulations of single-crystal experiments with a specific alloy are presented in Section 6.

2 Main ingredients: free energy and dissipation energy

As outlined in Introduction, mechanisms through which the material stores and dissipates energy are determinative for inelastic response of SMAs. Thus, corresponding response functions are ultimately the main ingredients for any model.

The parent austenite in a stress-free configuration represents a natural state of the material. From a viewpoint of *continuum mechanics*, we can thus speak about a *reference configuration* of a specimen occupying a domain $\Omega \subset \mathbb{R}^3$ and, as usual, $y : \Omega \to \mathbb{R}^3$ denotes the *deformation* and $u : \Omega \to \mathbb{R}^3$ the *displacement*, related to each other by $y(x) = x + u(x)$, $x \in \Omega$. Hence *deformation gradient* equals $F = \nabla y = \mathrm{I} + \nabla u$, where $\mathrm{I} \in \mathbb{R}^{3\times 3}$ denotes the identity matrix and ∇ is the Lagrangean gradient operator.

2.1 Free energy

The specific energy stored in the inter-atomic links in the continuum $\hat\psi = \hat\psi(F, \theta)$ is phenomenologically described as a function of the deformation gradient F and, in anisothermal case, a temperature θ. The *frame-indifference*, i.e. $\hat\psi(F, \theta) = \hat\psi(RF, \theta)$ for any $R \in$SO(d), the group of orientation-preserving rotations, requires that $\hat\psi$ in fact depends only on the (right) Cauchy-Green stretch tensor $C := F^\top F$. By d, we denote the dimension of the specimen domain $\Omega \subset \mathbb{R}^d$, though physically relevant case is $d = 3$ only. As $F = \mathrm{I} + \nabla u$, we can express the specific stored energy in terms of the displacement gradient as

$$\psi = \psi(\nabla u, \theta) = \hat\psi(\mathrm{I} + \nabla u, \theta). \tag{1}$$

As ψ in (1) does not depend explicitly on x, this form describes single crystals only; generalization for polycrystals by letting ϕ depend on x in a piece-wise (=grain-wise) constant manner is, in principle, simple, see [30]. The *Piola-Kirchhoff stress* $\sigma : \mathbb{R}^{d\times d} \to \mathbb{R}^{d\times d}$ is given by $\sigma = \frac{\partial}{\partial(\nabla u)}\psi(\nabla u, \theta)$.

We will use a *St. Venant-Kirchhoff*-like form of the stored energy of each particular phase variants which allows for an explicit reference to measured data and can easily

be applied to various materials. We consider that the material can occur in L stress-free configurations that are determined by *distortion matrices* U_ℓ, $\ell = 1, ..., L$, which are independent of θ, i.e. thermal expansion is neglected.

The frame-indifferent free energy of particular phase(variant)s is considered as a function of *Green strain* tensor ε^ℓ related to the distortion of this phase(variant). In the simplest case (cf. [41, Sect.6.6], e.g.), one can consider a function quadratic in terms of ε^ℓ of the form

$$\hat\psi_\ell(F,\theta) = \sum_{i,j,k,l=1}^{d} \varepsilon^\ell_{ij}\mathcal{C}^\ell_{ijkl}\varepsilon^\ell_{kl} - c_\ell\theta\ln\Big(\frac{\theta}{\theta_0}\Big) + d_\ell, \qquad \varepsilon^\ell = \frac{(U_\ell^\top)^{-1}F^\top F U_\ell^{-1} - \mathrm{I}}{2}, \tag{2}$$

where $\mathcal{C}^\ell = \{\mathcal{C}^\ell_{ijkl}\}$ is the 4th-order tensor of elastic moduli satisfying the usual symmetry relations depending also on symmetry of the specific phase(variant) ℓ, θ is a temperature (sometimes considered as a parameter only), θ_0 a reference temperature, while c_ℓ the heat capacity of this phase(variant) and d_ℓ is some offset. The overall stored energy is assembled as

$$\hat\psi(F,\theta) := -k_{\mathrm{B}}\theta\ln\Big(\sum_{\ell=1}^{L} \mathrm{e}^{-\hat\psi_\ell(F,\theta)/(k_{\mathrm{B}}\theta)}\Big) \tag{3}$$

where k_{B} is the Boltzmann constant (related per unit volume). This option exhibits the expected *multi-well* character and is backed up by statistical physics.

Another form of $\hat\psi$, namely $\hat\psi := \min_\ell \hat\psi_\ell$, for θ as a fixed parameter, has been used in [3] for CuAlNi undergoing cubic/orthorhombic phase transformation (=PT) and in [1] for NiMnGa with cubic/tetragonal PT. However, the data required for this potential are available in many other alloys except the measurements of the elastic tensor $\mathcal{C}^\ell$ which are standardly done (with few exceptions) only for the austenite so that elastic response of the martensitic variants has to be extrapolated. The heat capacities c_ℓ are usually obtained experimentally, while the offsets d_ℓ are then to be fitted to get the agreement with energetical equilibrium between martensite and austenite at a specific temperature. Typically, heat capacity of austenite is larger than of martensite, which is just what causes SME.

Assuming each C^ℓ positive definite, the important property from the mathematical viewpoint of ϕ is the polynomial growth and the coercivity of $\psi(x,\cdot,\theta)$ in the sense

$$\exists c_1, c_0 > 0 \;\; \forall (F,\theta)\in\mathbb{R}^{d\times d}\times\mathbb{R}^+: \quad c_0|F|^p - 1 \le \psi(F,\theta) \le c_1(1+|F|^p) \tag{4}$$

with $p = 4$, and the uniform Lipschitz continuity of $\psi(x,F,\cdot)$:

$$\forall (F,\theta_1,\theta_2)\in\mathbb{R}^{d\times d}\times[\delta,+\infty)^2: \quad \big|\psi(F,\theta_1) - \psi(F,\theta_2)\big| \le l_\delta\big|\theta_1-\theta_2\big|. \tag{5}$$

2.2 Mesoscopic description: Young measures

On a mesoscopic level, we want to see an "averaged character" of fast oscillations of the deformation gradient of minimizing sequences to the stored energy $u \mapsto \int_\Omega \psi(x,\nabla u,\theta)\mathrm{d}x$.

This can be described by a probability measure ν_x on $\mathbb{R}^{d\times d}$ possibly depending on (i.e. being parameterized by) $x\in\Omega$; cf. e.g. [5, 6, 36, 39]. We then call $\nu=\{\nu_x\}_{x\in\Omega}$ a *Young measure* [53] if, in addition, $x\mapsto\nu_x$ is weakly measurable. Young measures form a subset of the linear space $L^\infty_{\rm w}(\Omega;{\rm rca}(\mathbb{R}^{d\times d}))\cong L^1(\Omega;C_0(\mathbb{R}^{d\times d}))^*$ where ${\rm rca}(\mathbb{R}^{d\times d})$ stands for Radon measures on $\mathbb{R}^{d\times d}$ and $C_0(\mathbb{R}^{d\times d})$ for compactly supported continuous functions on $\mathbb{R}^{d\times d}$. In our context, relevant Young measures are only those that are attainable by gradients, i.e. $\nu=$w*-$\lim_{k\to\infty}\{\delta_{\nabla u_k(x)}\}_{x\in\Omega}$ for some sequence in the Sobolev space $W^{1,p}(\Omega;\mathbb{R}^d)$ with p referring to the p-power growth/coercivity of $F\mapsto\psi(F,\theta)$; here, in view of (2), $p=4$. Let us denote by $G^p(\Omega;\mathbb{R}^{d\times d})$ the set of such parameterized measures. An example of a Young measure ν describing a so-called 1st-order *laminate* with a macroscopic deformation $u\in W^{1,p}(\Omega;\mathbb{R}^d)$ is

$$\begin{aligned}\nu=\{\nu_x\}_{x\in\Omega},\quad \nu_x=\xi_1(x)\delta_{F_1(x)}+\xi_2(x)\delta_{F_2(x)},\\ [\xi_1F_1+\xi_2F_2](x)=\nabla u(x),\quad F_1(x)-F_2(x)=a(x)\otimes n(x),\\ \xi_1(x),\xi_2(x)\geq0,\quad \xi_1(x)+\xi_2(x)=1,\quad a(x),n(x)\in\mathbb{R}^d.\end{aligned}\tag{6}$$

This process can be re-iterated: a 2nd-order laminate with the macroscopic deformation u as above is $\nu=\{\nu_x\}_{x\in\Omega}$, where

$$\begin{aligned}\nu_x=\xi_0(x)\xi_1(x)\delta_{F_1(x)}+\xi_0(x)(1-\xi_1(x))\delta_{F_2(x)}\\ +(1-\xi_0(x))\xi_2(x)\delta_{F_3(x)}+(1-\xi_0(x))(1-\xi_2(x))\delta_{F_3(x)}\ ,\end{aligned}\tag{7}$$

with (dropping for simplicity a dependence on x)

$$F_1-F_2=a_1\otimes n_1,\qquad F_3-F_4=a_2\otimes n_2\ ,\tag{8a}$$

$$\xi_1F_1+(1-\xi_1)F_2-\xi_2F_3-(1-\xi_2)F_4=a\otimes n\ ,\tag{8b}$$

$$\nabla u=\xi_0\xi_1F_1+\xi_0(1-\xi_1)F_2+(1-\xi_0)\xi_2F_3+(1-\xi_0)(1-\xi_2)F_4\tag{8c}$$

and $0\leq\xi_i\leq1$, $a_i,n_i\in\mathbb{R}^d$, $i\in\{0,1,2\}$. Analogously, we can get a laminate of an arbitrary order.

Unfortunately, not every $\nu\in G^p(\Omega;\mathbb{R}^{d\times d})$ is of the form of a laminate, or even cannot be attained by laminates, which can be interpreted that microstructures might be much more chaotic. This is connected with the famous Šverák's counterexample [49] that rank-one convexity does not imply quasiconvexity. Moreover, description of $G^p(\Omega;\mathbb{R}^{d\times d})$ is not possible in an efficient way, which is related with lack of efficient characterization of quasiconvex functions; cf. [22, 39]. Nevertheless, at least for theoretical analysis in Section 3, we can work with all possible microstructures, i.e. with the whole set $G^p(\Omega;\mathbb{R}^{d\times d})$.

Starting from [37], there are numerical studies involving gradient Young measures as e.g. [3, 23, 24] but, due to the mentioned impossibility of an efficient description of the whole set $G^p(\Omega;\mathbb{R}^{d\times d})$, they eventually have to deal with laminates of an order $\kappa\geq1$, let us denote this set as

$$G^{p,\kappa}_{\rm lam}(\Omega;\mathbb{R}^{d\times d}):=\big\{\nu\in G^p(\Omega;\mathbb{R}^{d\times d});\ \ \nu_x\text{ is a }\kappa\text{-order laminate for a.a. }x\in\Omega\big\}.\tag{9}$$

2.3 Dissipation energy

PT in SMAs is characterized by a specific dissipation which results to a hysteretic response in stress/strain/temperature diagrams. This is, to a large extent, *rate-independent, activated process* similar like standard slip plasticity in metals and proper modelling of the dissipation is equally important as the stored energy, in particular to model evolution. As the dissipation seems essentially influenced by various impurities and dislocations, there is even more phenomenology needed than for the stored energy. We follow an attempt to build such a *phenomenology* on a purely continuum-level model proposed in [45, Formula (33)], based on (to some extent simplified) standpoint that the amount of dissipated energy within the particular PT (here it is meant also M/M-transformation, i.e. of one variant of the martensite transforms to another, sometimes referred rather as a re-orientation of martensite) can be described by a single, phenomenologically given number (of the dimension J/m^3=Pa). This philosophy is to design at least the energetics in accord with experiments, if the activated PT dynamics cannot be understood in detail by more rigorous arguments, and has independently been adopted in physics, see [20, 50, 51]. For this, we need to identify the particular phase(variant)s and thus define a continuous mapping $\mathcal{L}:\Omega\times\mathbb{R}^{d\times d}\to\triangle_L$ where $\triangle_L:=\{\,\zeta\in\mathbb{R}^L\,;\ \zeta_\ell\geq 0,\ \ell=1,...,L,\ \sum_{i=1}^L\zeta_\ell=1\,\}$ is a simplex with L vertices. Like (1), we assume

$$\mathcal{L}(F)=\hat{\mathcal{L}}(\mathrm{I}+F),\quad\text{with }\hat{\mathcal{L}}:\mathbb{R}^{d\times d}\to\triangle_L. \tag{10}$$

Again, $\hat{\mathcal{L}}$ is related with the material itself and thus is expected to be frame indifferent. We have in mind that the components $\{\hat{\mathcal{L}}_1,...,\hat{\mathcal{L}}_L\}$ of $\hat{\mathcal{L}}=(\hat{\mathcal{L}}_1,\dots,\hat{\mathcal{L}}_L)^\top$ form a *partition of unity* on $\mathbb{R}^{d\times d}$ such that $\mathcal{L}_\ell(F)$ is equal 1 if F is in the ℓ-th phase, i.e. F is in a neighborhood of ℓ-th well $\mathrm{SO}(d)U_\ell$ of ψ (which can be identified according to the stretch tensor $F^\top F$ closed to $U_\ell^\top U_\ell$ like in [31, 33]). Of course, $\hat{\mathcal{L}}(F)$ in the (relative) interior of $\triangle_L$ indicates F in the spinodal region where no definite phase is specified. Hence λ plays the role of what is often called a vector of *order parameters* or a vector-valued *internal variable*. The concrete form of $\hat{\mathcal{L}}$ does not seem to be important as long as $\hat{\mathcal{L}}$ enjoys the above properties.

The phenomenology itself is considered through the choice of a "norm" on $\mathbb{R}^L$ (not necessarily Euclidean and even not symmetric), let us denote it by $|\cdot|_L$; its physical dimension will be Jm^{-3}=Pa. The desired meaning is to set up the specific energy $\mathcal{E}_{\ell k}$ needed for PT of a phase(variant) ℓ to k as $|e_\ell-e_k|_L$, where $e_\ell=(0,..,0,1,0,...0)\in\mathbb{R}^L$ is the unit vector with 1 at the position ℓ.

Referring to (10), *mesoscopic volume fractions* at a current "macroscopic" point $\lambda=\lambda(x)$ will then be naturally calculated as

$$\lambda(x):=[\mathcal{L}\bullet\nu](x):=\int_{\mathbb{R}^{d\times d}}\mathcal{L}(F)\nu_x(\mathrm{d}F). \tag{11}$$

In terms of the volume fractions, the (pseudo)potential of dissipative forces that corre-

sponds this phenomenology is

$$R(q) = R(u, \nu, \lambda) := \int_\Omega \left| \frac{\partial \lambda}{\partial t} \right|_L \mathrm{d}x. \tag{12}$$

This means, considering a process over the time interval $[t_1, t_2]$, the overall dissipated energy by all underwent PTs in the whole specimen Ω will be

$$\int_{t_1}^{t_2} \int_\Omega \left| \frac{\partial \lambda}{\partial t} \right|_L \mathrm{d}x\mathrm{d}t = \int_\Omega \operatorname*{Var}_{t\in[t_1,t_2]} \lambda(t, x)\, \mathrm{d}x \tag{13}$$

where the total variation "Var" with respect to the (possibly nonsymmetric) norm $|\cdot|_L$ counts which PTs (and how many times) has been undergone in the point x.

The phenomenological dissipated energies $\mathcal{E}_{\ell k}$ are then to be got from experiments, and/or model-fitting technique, and/or from some other more or less speculative considerations. Sometimes, some hint can be found in the literature, e.g. for Ti-Ni single crystal [50, p.331] uses $\mathcal{E}_{\ell k} = 4.7$MPa if either ℓ or k refers to austenite (i.e. energy for A/M PT) while $\mathcal{E}_{\ell k} = 0$ otherwise (i.e. M/M-reorientation is considered as nondissipative, which however is not completely true, of course).

Let us remark that a lightly different construction of $\hat{\mathcal{L}}$ but of a similar spirit, relying on particular PTs rather than particular phase(variant)s, has been used in [2].

The important property of R is that it satisfies the triangle inequality, i.e.

$$\forall q_1, q_2, q_3 \in Q: \qquad R(q_1 - q_3) \le R(q_1 - q_2) + R(q_2 - q_3), \tag{14}$$

which follows immediately from convexity and the homogeneity of degree 1.

3 Mesoscopic-level model

Therefore, the *mesoscopic configuration* will be a triple $q := (u, \nu, \lambda)$ of macroscopic displacement u, the microstructure ν, and the volume fraction λ, and the set Q of admissible configurations is

$$Q := \Big\{ (u, \nu, \lambda) \in W^{1,p}(\Omega; \mathbb{R}^d) \times \mathcal{G}^p(\Omega; \mathbb{R}^{d\times d}) \times L^\infty(\Omega; \mathbb{R}^L);\ \nabla u = \mathrm{I} \bullet \nu,\ \lambda = \mathcal{L} \bullet \nu \Big\}, \tag{15}$$

where $\bullet$ is defined as in (11) but now, additionally to $\mathcal{L}$, also the identity on $\mathrm{I} : \mathbb{R}^{d\times d} \to \mathbb{R}^{d\times d}$ is used.

3.1 Rate-dependent model

Neglecting any rate-dependent (i.e. here kinetic and viscous) effects, in [31], Mielke and Theil introduced a suitable and efficient definition of a solution to rate-independent processes generally applicable e.g. to plasticity, ferromagnetics, delamination, damage, and

to SMAs, too, cf. [29, 30, 32, 33] and for numerical study [11]. Mielke-Theil's definition plays merely with energetics of the process $q : [0,T] \to Q$, requiring, beside the initial condition $q(0) = q_0$, its *stability* (16a) and the *energy inequality* (16b) in the sense:

$$\forall\, t \;\; \forall \tilde{q} \in Q : \qquad G\big(t, q(t)\big) \le G(t,\tilde{q}) + R\big(q(t) - \tilde{q}\big), \tag{16a}$$

$$\forall\, t \ge s : \qquad G\big(t, q(t)\big) + \mathrm{Var}_R(q; s, t) \le G\big(s, q(s)\big) + \int_s^t \frac{\partial G}{\partial \vartheta}\big(\vartheta, q(\vartheta)\big)\,\mathrm{d}\vartheta \tag{16b}$$

where $\mathrm{Var}_R(q; s, t) := \mathrm{Var}_L(\lambda; s, t)$ is the total variation over the time interval $[s, t]$ of the process $q = (u, \nu, \lambda)$, cf. (25) below. Moreover, here in (16), we consider

$$G(t,q) = G(t,u,\nu,\lambda) = \begin{cases} V(t,q) & \text{if } q \in Q, \\ +\infty & \text{elsewhere} \end{cases} \tag{17}$$

is the Gibbs stored energy with $V = V(t,q)$ the stored energy postulated by

$$\begin{aligned} V(t,q) = V(t,u,\nu,\lambda) := \int_\Omega \Big(\psi(\cdot,\theta(t)) \bullet \nu\Big)\mathrm{d}x + \;\; \rho|\lambda|^r_{W^{\alpha,r}(\Omega;\mathbb{R}^L)} \\ + \frac{1}{2}\int_\Gamma \big(u(x) - u_{\mathrm{D}}(t,x)\big)^\top A(x)\big(u(x) - u_{\mathrm{D}}(t,x)\big)\mathrm{d}S \end{aligned} \tag{18}$$

with the specific stored energy ψ from (1) and $\theta = \theta(t)$ a given temperature regime, $A : \Gamma \to \mathbb{R}^{d\times d}$, with $A(x)$ symmetric, positive definite, $u_{\mathrm{D}} : [0,T] \times \Gamma \to \mathbb{R}^d$ determining a prescribe loading regime, and $\mathrm{Var}_R(q; s, t)$ is the total variation of the process q over the time interval $[s, t]$ with respect to the dissipation potential R, cf. (25) below. Again, $\bullet$ in (18) is defined as in (11) but now with $\psi(\cdot,\cdot,\theta(t))$ instead of $\mathcal{L}$. Thorough this contribution, we will assume $p > 2d/(d+1)$ so that the traces on Γ of $W^{1,p}(\Omega;\mathbb{R}^d)$-functions are (even "compactly") in $L^2(\Gamma;\mathbb{R}^d)$ and therefore the boundary term in (18) has a good sense. In Sect. 2.1, we considered $p = 4$ and $d = 3$ which certainly satisfies this restriction. Furthermore, $\rho > 0$ in (18) denotes a (small) regularizing parameter expressing that spatial variations of volume fractions λ has a certain (small) energy, and $r > 1$. The semi-norm in the Sobolev-Slobodetskiĭ space $W^{\alpha,r}(\Omega;\mathbb{R}^L)$ can be considered as

$$\big|\lambda\big|_{W^{\alpha,r}(\Omega;\mathbb{R}^L)} := \left(\frac{1}{4}\int_\Omega\int_\Omega \frac{\big|\lambda(x) - \lambda(\xi)\big|^r}{|x-\xi|^{d+r\alpha}}\,\mathrm{d}\xi\mathrm{d}x\right)^{1/r}, \tag{19}$$

for a fixed parameter $0 < \alpha < 1 - d(r-1)/r$. Such a regularizing term in (18) corresponds to the (square of the) norm in the Sobolev-Slobodetskiĭ space $W^{\alpha,r}(\Omega,\mathbb{R}^L)$ which is compactifying if $\alpha > 0$ and which, for α small enough as indicated, allows us to use piecewise constant approximation of λ which has necessarily discontinuities on $(d-1)$-dimensional manifolds. Let us remark that this regularization (18) by a higher-order term in λ with $\rho > 0$ can be interpreted [30, 46] as a limit from the Ericksen-Timoshenko model scrutinized in [43, 44]. Gradients of mesoscopic volume fractions has already been used in Frémond's model [15, p.364] or also in [30]; this is, however, not suitable for piecewise

constant finite-element approximation. The nonlocal term used here in (18) was proposed in the case $d = 1$ by Ren, Rogers, and Truskinovsky [43, 44] with either positive or also, for different purposes, non-positive kernels, and in multidimensional context in [2].

Such a model has been scrutinized in [30] for an isothermal case (i.e. θ constant), and it has been proved that there is a solution process $q : [0,T] \to Q$ satisfying (16a) and (16b), even as an equality, and also an initial condition $q(0) = q_0$, and such that, moreover, $u(\cdot)$, $\lambda(\cdot)$, and $G(\cdot, q(\cdot))$ are measurable in time. The assumptions involved, in particular, stability of the initial state q_0, loading $W^{1,1}$-smoothness in time of the loading $u_{\rm D}$, a certain "non-buckling" hypothesis (see (64) below), and the regularizing gradient term $\int_\Omega |\nabla\lambda|^2 {\rm d}x$ has been used in (18) instead of the Sobolev-Slobodetskiĭ term $\big|\lambda\big|^r_{W^{\alpha,r}(\Omega;\mathbb{R}^L)}$ here. A semidiscretization in time has been used, leading to a recursion of minimization problems involving the set of gradient Young measures $\mathcal{G}^p(\Omega;\mathbb{R}^{d\times d})$. While the "non-buckling" hypothesis seems to be avoidable if a more sophisticated technique [14] would be exploited, the efficient approximation procedure which guarantees convergence of the model in [30] based on the regularized V was not obvious so far and is one of the goal of this contribution.

3.2 Volume-fraction solution

The definition from Section 3.1 is based on the set $\mathcal{G}^p(\Omega;\mathbb{R}^{d\times d})$ which cannot be handled explicitly. Anyhow, the numerical simulations presented below show a certain convergence at least in some situations and nice applicability, which calls for some theory to support it rigorously. A certain way is to weaken the definition of the solution to involve only some quantities, here the overall stored energy and power of external loading, and the distributed volume fraction, while the macroscopic displacement u and the Young measure ν are not involved explicitly. Let us first denote

$$Q(\lambda) := \big\{(u,\nu) \in W^{1,p}(\Omega;\mathbb{R}^d) \times \mathcal{G}^p(\Omega;\mathbb{R}^{d\times d}) \ ; \ (u,\nu,\lambda) \in Q\big\} \ . \tag{20}$$

Then we define the *"condensed" stored energy*

$$\mathfrak{G}(t,\lambda) := \inf_{(u,\nu)\in Q(\lambda)} G(t,u,\nu,\lambda), \tag{21}$$

and abbreviate the set of admissible volume-fraction distributions as

$$\Lambda := \Big\{\lambda \in L^\infty(\Omega;\mathbb{R}^L); \quad \exists\, \nu \in G^p(\Omega;\mathbb{R}^{d\times d}), \quad \lambda = \mathcal{L} \bullet \nu\Big\}. \tag{22}$$

Also, let us abbreviate

$$\mathfrak{R}(\lambda) := \int_\Omega \big|\lambda(x)\big|_L {\rm d}x. \tag{23}$$

Then (16) turns into

$$\forall\, t \ \ \forall \tilde\lambda \in \Lambda : \qquad \mathfrak{G}\big(t,\lambda(t)\big) \le \mathfrak{G}(t,\tilde\lambda) + \mathfrak{R}\big(\lambda(t,\cdot) - \tilde\lambda\big), \tag{24a}$$

$$\forall\, t \ge s : \qquad \mathfrak{G}\big(t,\lambda(t)\big) + {\rm Var}_L(\lambda;s,t) \le \mathfrak{G}\big(s,\lambda(s)\big) + \int_s^t \frac{\partial \mathfrak{G}}{\partial \vartheta}\big(\vartheta,\lambda(\vartheta)\big)\,{\rm d}\vartheta \tag{24b}$$

where $\mathrm{Var}_L(\lambda;s,t)$ is the total variation of the process λ over the time interval $[s,t]$ with respect to the dissipation potential (12), i.e.

$$\mathrm{Var}_L(\lambda;s,t)=\sum_{i=1}^{I}\int_\Omega \big|\lambda(t_i,x)-\lambda(t_{i-1},x)\big|_L\mathrm{d}x \tag{25}$$

where the summation is taken over all partition $s=t_0<t_1<...<t_I=t$, $I\in\mathbb{N}$.

4 Approximate scheme

As the set $G^p(\Omega;\mathbb{R}^{d\times d})$ cannot be explicitly implemented, instead we will work with a smaller set $G^{p,k}_{\rm lam}(\Omega;\mathbb{R}^{d\times d})$ from (9). This brings, however, a necessity to treat the relation $\lambda=\mathcal{L}\bullet\nu$ by a "tolerance" because, due to the compactness in λ's caused by the regularizing nonlocal ϱ-term in (18), it behaves like a constraint which, if treated without any tolerance, might destroy the convergence. For this, we make a penalization of the constraint $\lambda=\mathcal{L}\bullet\nu$ in a space to which $L^\infty(\Omega;\mathbb{R}^L)\cap W^{\alpha,r}(\Omega;\mathbb{R}^L)$ is embedded compactly, e.g. the space $H^{-1}(\Omega;\mathbb{R}^L):=W^{-1,2}(\Omega;\mathbb{R}^L)$. It should be emphasized that this additional regularization is just to guarantee the convergence and does not affect the original problem.

To construct approximate solutions, we consider a time step $\tau>0$, assuming T/τ integer and also that $\tau\to0$ in such a way that the equidistant partitions will be nested; for example, the reader can think about a sequence of time steps $\tau=2^{-k}T$ for $k\in\mathbb{N}$. Besides, we will employ the finite-element method, assuming that Ω is a polyhedral domain triangulated by simplectic triangulation, denoted by $\mathcal{T}_h$, $h>0$ a mesh parameter, i.e. $h=\max_{S\in\mathcal{T}_h}\mathrm{diam}(S)$. Also, we consider a countable set of h's and assume that $\mathcal{T}_{h_1}$ is a refinement of $\mathcal{T}_{h_2}$ if $h_2\geq h_1>0$.

We fix an order of lamination $\kappa\geq1$ in (9). For $\tau>0$ and $h>0$ fixed, and for a regularizing penalty parameter $\varepsilon>0$, we consider the fully implicit formula based on the following recursive increment formula: we put $q^0_\tau=q_0$ a given initial condition, and, for $k=1,...,T/\tau$ we define $q^{\varepsilon,k}_{\tau,h}$ to be a solution of the minimization problem

$$\left.\begin{array}{ll}\text{Minimize} & V(k\tau,q)+R(q{-}q^{k-1})+\frac{1}{\varepsilon}\big\|\lambda{-}\mathcal{L}\bullet\nu\big\|^2_{H^{-1}(\Omega;\mathbb{R}^L)}\\ \text{subject to} & q=(u,\nu,\lambda),\quad u\in W^{1,p}(\Omega;\mathbb{R}^d),\\ & \nabla u=\mathrm{I}\bullet\nu,\quad \lambda(x)\in\triangle_L\quad\text{for a.a. } x\in\Omega\\ & \nu\in G^{p,\kappa}_{\rm lam}(\Omega;\mathbb{R}^{d\times d})\ \text{ element-wise constant on } \mathcal{T}_h,\\ & \lambda\in L^\infty(\Omega;\mathbb{R}^L)\ \text{ element-wise constant on } \mathcal{T}_h.\end{array}\right\}\tag{26}$$

For $k=0$, we naturally put $q^{\varepsilon,k}_{\tau,h}=q_0$, a given initial condition. As R involves only λ, the component λ_0 of $q_0=(u_0,\nu_0,\lambda_0)$ is what plays role. Note that each admissible u in (26) is inevitably element-wise affine on $\mathcal{T}_h$.

As (26) is a minimization problem on a finite-dimensional manifold with a functional coercive on this manifold, a solution to (26) does exist. Let us define $q^\varepsilon_{\tau,h}(t) := q^{\varepsilon,k}_{\tau,h}$ if $t \in ((k-1)\tau, k\tau]$. The following assertion states a-priori estimates for the λ-component of $q^\varepsilon_{\tau,h}$, i.e. $\lambda^\varepsilon_{\tau,h}$. For this, let us re-define the needed quantities in terms of λ as follows:

$$\mathfrak{G}^\varepsilon_h(t,\lambda) := \inf_{\substack{(u,\nu)\in W^{1,p}(\Omega;\mathbb{R}^d)\times G^{p,\kappa}_{\rm lam}(\Omega;\mathbb{R}^{d\times d}) \\ \nu \text{ is element-wise constant on } \mathcal{T}_h \\ \nabla u = \mathrm{I}\bullet\nu}} V(t,u,\nu,\lambda) + \frac{1}{\varepsilon}\big\|\lambda - \mathcal{L}\bullet\nu\big\|^2_{H^{-1}(\Omega;\mathbb{R}^L)}, \tag{27}$$

$$\mathfrak{G}^\varepsilon_{\tau,h}(t,\lambda) := \mathfrak{G}^\varepsilon_h(k\tau,\lambda) \qquad \text{for } t\in((k-1)\tau,k\tau], \tag{28}$$

Note that this definition admits also $t=0$; then $k=0$. The component $\lambda^{\varepsilon,k}_{\tau,h}$ from $q^{\varepsilon,k}_{\tau,h}$ solving (26) now solves the problem

$$\left.\begin{array}{l} \text{Minimize} \quad \mathfrak{G}^\varepsilon_h(k\tau,\lambda) + \mathfrak{R}(\lambda - \lambda^{\varepsilon,k-1}_{\tau,h}) \\ \text{subject to} \ \ \lambda \in \Lambda_h \end{array}\right\} \tag{29}$$

with $\lambda^{\varepsilon,k}_{\tau,h} = \lambda_0$, where $\mathfrak{R}$ is defined in (23) and

$$\Lambda_h := \big\{\lambda\in L^\infty(\Omega;\mathbb{R}^L) \text{ element-wise constant on } \mathcal{T}_h : \lambda(x)\in\triangle_L \text{ for a.a. } x\in\Omega\big\}. \tag{30}$$

Proposition 4.1 *Let*

$$u_{\rm D} \in W^{1,1}(0,T;L^2(\Gamma;\mathbb{R}^d)), \tag{31a}$$

$$A\in L^\infty(\Gamma;\mathbb{R}^{d\times d}), \quad A(\cdot) \text{ positive semidefinite a.e. on } \Gamma$$
$$A(\cdot) \text{ positive definite on } \Gamma_0\subset\Gamma,\ \mathrm{meas}_{d-1}(\Gamma_0)>0, \tag{31b}$$

$$\theta\in W^{1,1}(0,T), \quad \theta(\cdot)\ge\delta>0, \tag{31c}$$

and let the initial state is a homogeneous equilibrium with respect to the initial loading in the sense

$$u_0 = 0, \quad u_{\rm D}(0,\cdot)=0, \quad \exists \text{ homogeneous } \nu \text{ minimizing } \psi(\cdot,\theta(0)), \quad \lambda_0 = \mathcal{L}\bullet\nu. \tag{32}$$

Then $\lambda^\varepsilon_{\tau,h}$ is stable in the sense

$$\forall\tilde\lambda\in\Lambda_h: \qquad \mathfrak{G}^\varepsilon_h\big(t,\lambda^\varepsilon_{\tau,h}(t)\big) \le \mathfrak{G}^\varepsilon_h\big(t,\tilde\lambda\big) + \mathfrak{R}\big(\lambda^\varepsilon_{\tau,h}(t)-\tilde\lambda\big) \tag{33}$$

for all $t\in[0,T]$, and satisfies the two-sided discrete energy inequality

$$\begin{aligned}\int_0^t \frac{\partial\mathfrak{G}^\varepsilon_h}{\partial\vartheta}\big(\vartheta,\lambda^\varepsilon_{\tau,h}(\vartheta)\big)\mathrm{d}\vartheta \ &\le\ \mathfrak{G}^\varepsilon_{\tau,h}\big(t,\lambda^\varepsilon_{\tau,h}(t)\big) + \mathrm{Var}_L(\lambda^\varepsilon_{\tau,h};0,t) \\ &-\ \mathfrak{G}^\varepsilon_{\tau,h}(0,\lambda_0) \le \int_0^t \frac{\partial\mathfrak{G}^\varepsilon_h}{\partial\vartheta}\big(\vartheta,\lambda^\varepsilon_{\tau,h}(\vartheta-\tau)\big)\mathrm{d}\vartheta,\end{aligned} \tag{34}$$

for $t=\tau k$, $k=0,1,...,T/\tau$. Also, the following a-priori estimates hold:

$$\big\|\lambda^\varepsilon_{\tau,h}\big\|_{BV(0,T;L^1(\Omega;\mathbb{R}^L))\,\cap\, L^\infty(0,T;L^\infty(\Omega;\mathbb{R}^L))\,\cap\, L^\infty(0,T;W^{\alpha,r}(\Omega;\mathbb{R}^L))} \le C_1, \tag{35}$$

$$\big\|\mathcal{G}^\varepsilon_{\tau,h}\big\|_{BV(0,T)} \le C_2 \qquad \text{where } \mathcal{G}^\varepsilon_{\tau,h}(t) := \mathfrak{G}^\varepsilon_{\tau,h}(t,\lambda^\varepsilon_{\tau,h}(t)). \tag{36}$$

Proof. As to the discrete stability condition, as in [33, Thm.3.4], by using successively that $\lambda_{\tau,h}^{\varepsilon,k}$ is a minimizer (cf. (26)) and the triangle inequality (14) for R (written in term of $\mathfrak{R}$), we obtain

$$\begin{aligned}\mathfrak{G}_h^\varepsilon(k\tau,\lambda_{\tau,h}^{\varepsilon,k}) &\le \mathfrak{G}_h^\varepsilon(k\tau,\tilde\lambda)+\mathfrak{R}(\tilde\lambda-\lambda_{\tau,h}^{\varepsilon,k-1})-\mathfrak{R}(\lambda_{\tau,h}^{\varepsilon,k}-\lambda_{\tau,h}^{\varepsilon,k-1})\\ &\le \mathfrak{G}_h^\varepsilon(k\tau,\tilde\lambda)+\mathfrak{R}(\tilde\lambda-\lambda_{\tau,h}^{\varepsilon,k})\end{aligned} \tag{37}$$

for any $k=1,...,K=T/\tau$. In view of the definition of $\lambda_{\tau,h}^\varepsilon$ and $\mathfrak{G}_{\tau,h}^\varepsilon$, it just means (33).

The proof of the energy inequality (34) follows as in [33, eqn. (2.12)]. Since $\lambda_{\tau,h}^{\varepsilon,k}$ minimizes the condensed energy

$$\lambda\mapsto\mathfrak{G}_h^\varepsilon(k\tau,\lambda)+\mathfrak{R}(\lambda-\lambda_{\tau,h}^{\varepsilon,k-1}), \tag{38}$$

over Λ_h, we deduce, by inserting $\lambda=\lambda_{\tau,h}^{\varepsilon,k-1}$, the estimate

$$\begin{aligned}&\mathfrak{G}_h^\varepsilon(k\tau,\lambda_{\tau,h}^{\varepsilon,k})-\mathfrak{G}_h^\varepsilon\big((k{-}1)\tau,\lambda_{\tau,h}^{\varepsilon,k-1}\big)+\mathfrak{R}\big(\lambda_{\tau,h}^{\varepsilon,k}{-}\lambda_{\tau,h}^{\varepsilon,k-1}\big)\\ &\quad\le\mathfrak{G}_h^\varepsilon\big(k\tau,\lambda_{\tau,h}^{\varepsilon,k-1}\big)-\mathfrak{G}_h^\varepsilon\big((k{-}1)\tau,\lambda_{\tau,h}^{\varepsilon,k-1}\big)=\int_{(k-1)\tau}^{k\tau}\frac{\partial\mathfrak{G}_h^\varepsilon}{\partial\vartheta}\big(\vartheta,\lambda_{\tau,h}^{\varepsilon,k-1}\big)\mathrm{d}\vartheta.\end{aligned} \tag{39}$$

Here we used that, by (5) and the $W^{1,1}$-smoothness of both θ and $u_{\rm D}$, $\frac{\partial}{\partial t}\mathfrak{G}_h^\varepsilon$ does exist and is integrable, cf. (42) below.

As to the left-hand part of (34), like in [32, Theorem 4.1] by the stability (37) written for $\lambda_{\tau,h}^{\varepsilon,k-1}$, we can see that $\lambda_{\tau,h}^{\varepsilon,k-1}$ minimizes the functional $\lambda\mapsto\mathfrak{G}_h^\varepsilon((k{-}1)\tau,\lambda)+\mathfrak{R}(\lambda{-}\lambda_{\tau,h}^{\varepsilon,k-1})$, and therefore, by inserting $\lambda=\lambda_{\tau,h}^{\varepsilon,k}$, we find

$$\begin{aligned}&\mathfrak{G}_h^\varepsilon\big(k\tau,\lambda_{\tau,h}^{\varepsilon,k}\big)-\mathfrak{G}_h^\varepsilon\big((k{-}1)\tau,\lambda_{\tau,h}^{\varepsilon,k-1}\big)+\mathfrak{R}\big(\lambda_{\tau,h}^{\varepsilon,k}{-}\lambda_{\tau,h}^{\varepsilon,k-1}\big)\\ &\quad\ge\mathfrak{G}_h^\varepsilon\big(k\tau,\lambda_{\tau,h}^{\varepsilon,k}\big)-\mathfrak{G}_h^\varepsilon\big((k{-}1)\tau,\lambda_{\tau,h}^{\varepsilon,k}\big)=\int_{(k-1)\tau}^{k\tau}\frac{\partial\mathfrak{G}_\langle^\varepsilon}{\partial\vartheta}\big(\vartheta,\lambda_{\tau,h}^{\varepsilon,k}\big)\mathrm{d}\vartheta.\end{aligned} \tag{40}$$

By summing (39) and (40) for $k=1,...,t/\tau$, we obtain (34). For $k=1$, we used that, because of (32), $\lambda_{\tau,h}^{\varepsilon,0}=\lambda_0$ is stable in the sense that

$$\forall\tilde\lambda\in\Lambda_h:\qquad\mathfrak{G}_h^\varepsilon\big(0,\lambda_0\big)\le\mathfrak{G}_h^\varepsilon\big(0,\tilde\lambda\big)+\mathfrak{R}\big(\lambda_0-\tilde\lambda\big) \tag{41}$$

For the a-priori estimates, we need $\partial\mathfrak{G}_\langle^\varepsilon/\partial\sqcup$ bounded. By (5),

$$\Big|\frac{\partial\mathfrak{G}_\langle^\varepsilon}{\partial\vartheta}\big(\vartheta,\lambda\big)\Big|\le l_\delta|\Omega|\Big|\frac{\mathrm{d}\theta}{\mathrm{d}\vartheta}\Big|+\int_\Gamma|A(u-u_{\rm D})|\,\Big|\frac{\partial u_{\rm D}}{\partial\vartheta}\Big|\mathrm{d}S. \tag{42}$$

The BV-bound in the estimate (35) then follows directly from (39), while the L^∞-bound is obvious since $\lambda_{\tau,h}^\varepsilon(t,x)\in\triangle_L$ for a.a. $(t,x)\in[0,T]\times\Omega$ and $\triangle_L\subset\mathbb{R}^L$ is bounded, and eventually by summing (39) for $k=1,2,....$, we get $\mathfrak{G}_{\tau,h}^\varepsilon(t,\lambda_{\tau,h}^\varepsilon(t))$ bounded from above

uniformly in $t\in[0,T]$ so that, in view of (18), the bound for $|\lambda^\varepsilon_{\tau,h}(t)|_{W^{\alpha,r}(\Omega;\mathbb{R}^L)}$ uniform in $t\in[0,T]$ follows.

By (39) and (40) and also by using (42),

$$\begin{aligned}\mathrm{Var}(\mathcal{G}^\varepsilon_{\tau,h};0,T) &= \sum_{k=1}^{T/\tau}\left|\mathfrak{G}^\varepsilon_h(k\tau,\lambda^{\varepsilon,k}_{\tau,h})-\mathfrak{G}^\varepsilon_h((k{-}1)\tau,\lambda^{\varepsilon,k-1}_{\tau,h})\right|\\ &\le \sum_{k=1}^{T/\tau}\max\Big(\int_{(k-1)\tau}^{k\tau}\frac{\partial\mathfrak{G}^\varepsilon_h}{\partial\vartheta}\big(\vartheta,\lambda^{\varepsilon,k-1}_{\tau,h}\big)\mathrm{d}\vartheta,\\ &\qquad \mathfrak{R}\big(\lambda^{\varepsilon,k}_{\tau,h}{-}\lambda^{\varepsilon,k-1}_{\tau,h}\big)+\int_{(k-1)\tau}^{k\tau}\Big|\frac{\partial\mathfrak{G}^\varepsilon_\zeta}{\partial\vartheta}\big(\vartheta,\lambda^{\varepsilon,k}_{\tau,h}\big)\Big|\mathrm{d}\vartheta\Big)\\ &\le l_\delta|\Omega|\,\big\|\theta\big\|_{W^{1,1}(0,T)}+\mathrm{Var}_L(\lambda^\varepsilon_{\tau,h};0,T)\\ &+ \big\|A(u-u_{\mathrm{D}})\big\|_{L^\infty(\Omega;L^2(\Gamma;\mathbb{R}^d))}\big\|u_{\mathrm{D}}\big\|_{W^{1,1}(0,T;L^2(\Gamma;\mathbb{R}^d))}\end{aligned}\tag{43}$$

which proves a bound for $\|\mathcal{G}^\varepsilon_{\tau,h}\|_{BV(0,T)}:=\int_0^T|\mathcal{G}^\varepsilon_{\tau,h}|\mathrm{d}t+\mathrm{Var}(\mathcal{G}^\varepsilon_{\tau,h};0,T)$, i.e. (36). □

We say that a collection of triangulations $\{\mathcal{T}_h\}_{h>0}$ is *regular* if there is $c>0$ such that, for every finite element $E\in\mathcal{T}_h$, $r_E/\ell_E>c$ for any $h>0$ where ℓ_E is the length of the longest edge (side) and r_E is the radius of the largest ball inscribed into E. We will need

$$W^{1,1}(\Omega;\mathbb{R}^L)\subset W^{\alpha,r}(\Omega;\mathbb{R}^L)\Subset L^1(\Omega;\mathbb{R}^L),\tag{44}$$

the latter embedding being compact. This indeed holds if

$$0<\alpha<1-\frac{r-1}{r}d\quad\text{ and }\quad 1<r<\frac{d}{d-1},\tag{45}$$

the latter condition guaranteeing just existence of some α satisfying the former condition.

Lemma 4.2 *If (45) holds, then*

$$\forall\lambda\in\Lambda\ \ \exists\{\lambda_h\}_{h>0}:\quad \lambda_h\in\Lambda_h,\quad \lambda_h\to\lambda\ \ \textit{in } W^{\alpha,r}(\Omega;\mathbb{R}^L).\tag{46}$$

Proof. We know that $C^1(\Omega;\mathbb{R}^L)$ is dense in $W^{\alpha,r}(\Omega;\mathbb{R}^L)$. Each $\tilde\lambda\in C^1(\Omega;\mathbb{R}^L)$ can further be approximated by $\lambda_h\in\Lambda_h$ in the norm of $W^{\alpha,r}(\Omega;\mathbb{R}^L)$ with an arbitrary accuracy if $h>0$ is small enough. Indeed, considering integral averages over each element, we get an approximation λ_h converging to $\tilde\lambda$ in $L^1(\Omega;\mathbb{R}^L)$ and, moreover, has the total variation bounded uniformly with respect to $h>0$. By (45) and the standard Sobolev embedding theorem, (44) holds and this former embedding in (44) is inherited by the respective biduals, i.e. $W^{1,1}(\Omega;\mathbb{R}^L)^{**}\subset W^{\alpha,r}(\Omega;\mathbb{R}^L)^{**}\cong W^{\alpha,r}(\Omega;\mathbb{R}^L)$ compactly because $r>1$ is assumed so that $W^{\alpha,r}(\Omega;\mathbb{R}^L)$ is reflexive. As $\{\lambda_h\}_{h>0}$ is bounded in $\mathrm{BV}(\Omega;\mathbb{R}^L)$, by the Hahn-Banach extension argument it can be considered as embedded into $W^{1,1}(\Omega;\mathbb{R}^L)^{**}$

with keeping the same norm, hence it is compact in $W^{\alpha,r}(\Omega;\mathbb{R}^L)$. Besides, the conventional smoothing procedure as well as the mentioned integral averaging keep values inside the convex hull of values of the original λ, i.e. $\lambda_h(x)\in\triangle_L$ can indeed be expected. $\square$

To prove the convergence, we state the following approximation property of $\mathfrak{G}$ by the sequence $\{\mathfrak{G}_h^\varepsilon\}_{\varepsilon,h>0}$; in fact, it is a combination of the Γ-like and the Mosco-like convergences $\mathfrak{G}_h^\varepsilon\to\mathfrak{G}$.

Lemma 4.3 *Let in addition to (31), also*

$$\lim_{t_h\to t}\frac{\partial u_{\rm D}}{\partial t}(t_h,\cdot)=\frac{\partial u_{\rm D}}{\partial t}(t,\cdot)\qquad \text{a.e. in }\Omega, \tag{47a}$$

$$\left|\frac{\partial u_{\rm D}}{\partial t}(t,\cdot)\right|\le g(\cdot)\qquad \text{a.e. in }\Omega\text{ for any }t\in[0,T] \tag{47b}$$

for some $g\in L^2(\Gamma)$. Moreover, if the nested collection of triangulations $\{\mathcal{T}_h\}_{h>0}$ is regular and if $\theta\in C([0,T])$, then

$$\liminf_{\substack{\varepsilon\to0\\ \lambda^\varepsilon\to\lambda\text{ weakly}\\ \text{in }W^{\alpha,r}(\Omega;\mathbb{R}^L)}}\ \liminf_{\substack{\lambda_h\in\Lambda_h,\quad t_h\to t,\quad h\to0\\ \lambda_h^\varepsilon\to\lambda^\varepsilon\text{ weakly}\\ \text{in }W^{\alpha,r}(\Omega;\mathbb{R}^L)}}\mathfrak{G}_h^\varepsilon(t_h,\lambda_h^\varepsilon)\ge\mathfrak{G}(t,\lambda), \tag{48}$$

$$\lim_{\varepsilon\to0}\ \limsup_{\substack{\lambda_h\to\lambda\text{ in }W^{\alpha,r}(\Omega;\mathbb{R}^L)\\ \lambda_h\in\Lambda_h,\quad t_h\to t,\quad h\to0}}\mathfrak{G}_h^\varepsilon(t_h,\lambda_h)\le\mathfrak{G}(t,\lambda) \tag{49}$$

for all $(t,\lambda)\in[0,T]\times\Lambda$.

Proof. Let us define

$$\mathfrak{G}^\varepsilon(t,\lambda):=\inf_{\substack{(u,\nu)\in W^{1,p}(\Omega;\mathbb{R}^d)\times G^p(\Omega;\mathbb{R}^{d\times d})\\ \nabla u=\mathrm{I}\bullet\nu,\ \lambda(x)\in\triangle_L\text{for a.a. }x\in\Omega}}V(t,u,\nu,\lambda)+\frac{1}{\varepsilon}\big\|\lambda-\mathcal{L}\bullet\nu\big\|^2_{H^{-1}(\Omega;\mathbb{R}^L)}. \tag{50}$$

Consider $\lambda_h^\varepsilon\to\lambda^\varepsilon$ weakly in $W^{\alpha,r}(\Omega;\mathbb{R}^L)$, $\lambda_h^\varepsilon\in\Lambda_h$, and $t_h\to t$ for $h\to0$. As $\{\lambda_h^\varepsilon\}_{h>0}$ is bounded also in $L^\infty(\Omega;\mathbb{R}^L)$, $\lambda_h^\varepsilon\to\lambda^\varepsilon$ weakly* in $L^\infty(\Omega;\mathbb{R}^L)$, too. Moreover, let us take $(u_h^\varepsilon,\nu_h^\varepsilon)\in W^{1,p}(\Omega;\mathbb{R}^d)\times G^{p,\kappa}_{\rm lam}(\Omega;\mathbb{R}^{d\times d})$, u_h^ε piecewise affine on $\mathcal{T}_h$ and ν_h^ε piecewise constant on $\mathcal{T}_h$, which realizes the infimum in (27) for $(t_h,\lambda_h^\varepsilon)$ in place of (t,λ). Such a couple $(u_h^\varepsilon,\nu_h^\varepsilon)$ does exist due to the coercivity (4) because, having λ and κ fixed, the admissible pairs (u,ν) for the minimization problem in (27) represent a finite-dimensional manifold. By the mentioned coercivity (4), all the sequences $\{u_h^\varepsilon\}_{h>0}$ and $\{\nu_h^\varepsilon\}_{h>0}$ are bounded in $W^{1,p}(\Omega;\mathbb{R}^d)$ and $L^\infty_{\rm w}(\Omega;{\rm rca}(\mathbb{R}^{d\times d}))$, respectively, hence, in terms of a subsequence, $u_h^\varepsilon\to u^\varepsilon$ weakly in $W^{1,p}(\Omega;\mathbb{R}^d)$ and $\nu_h^\varepsilon\to\mu^\varepsilon$ weakly* in $L^\infty_{\rm w}(\Omega;{\rm rca}(\mathbb{R}^{d\times d}))$

. By compactness of the trace operator $u \mapsto u|_\Gamma : W^{1,p}(\Omega;\mathbb{R}^d) \to L^2(\Gamma;\mathbb{R}^d)$ (here the restriction $p > 2d/(d+1)$ is used), we have

$$\begin{aligned}
\liminf_{h\to 0} \int_\Omega \psi(\cdot,\cdot,\theta(t_h)) \bullet \nu_h^\varepsilon \mathrm{d}x + \rho|\lambda_h^\varepsilon|^r_{W^{\alpha,r}(\Omega;\mathbb{R}^L)} + \frac{1}{\varepsilon}\big\|\lambda_h^\varepsilon - \mathcal{L}\bullet\nu_h^\varepsilon\big\|^2_{H^{-1}(\Omega;\mathbb{R}^L)} \\
+\frac{1}{2}\int_\Gamma \big(u_h^\varepsilon(x) - u_{\mathrm{D}}(t_h,x)\big)^\top A(x)\big(u_h^\varepsilon(x) - u_{\mathrm{D}}(t_h,x)\big)\mathrm{d}S \\
\ge \int_\Omega \psi(\cdot,\cdot,\theta(t_h)) \bullet \nu^\varepsilon \mathrm{d}x + \rho|\lambda^\varepsilon|^r_{W^{\alpha,r}(\Omega;\mathbb{R}^L)} + \frac{1}{\varepsilon}\big\|\lambda^\varepsilon - \mathcal{L}\bullet\mu^\varepsilon\big\|^2_{H^{-1}(\Omega;\mathbb{R}^L)} \\
+\frac{1}{2}\int_\Gamma \big(u^\varepsilon(x) - u_{\mathrm{D}}(t,x)\big)^\top A(x)\big(u^\varepsilon(x) - u_{\mathrm{D}}(t,x)\big)\mathrm{d}S \ge \mathfrak{G}^\varepsilon(t,\lambda). \qquad (51)
\end{aligned}$$

Note that the inequality in (51) is due to the term $|\cdot|^r_{W^{\alpha,r}(\Omega;\mathbb{R}^L)}$, while the limit in the other terms is just by their continuity. This shows that

$$\liminf_{\substack{\lambda_h^\varepsilon\to\lambda^\varepsilon \text{ weakly in } W^{\alpha,r}(\Omega;\mathbb{R}^L)\\ \lambda_h^\varepsilon\in\Lambda_h,\quad t_h\to t,\quad h\to 0}} \mathfrak{G}_h^\varepsilon(t_h,\lambda_h^\varepsilon) \ge \mathfrak{G}^\varepsilon(t,\lambda^\varepsilon) \qquad (52)$$

for $\varepsilon > 0$ fixed. Eventually,

$$\liminf_{\substack{\varepsilon\to 0,\ \lambda_\varepsilon\to\lambda \text{ weakly}\\ \text{in } W^{\alpha,r}(\Omega;\mathbb{R}^L)}} \mathfrak{G}^\varepsilon(t,\lambda^\varepsilon) \ge \liminf_{\substack{\varepsilon\to 0,\ \lambda_\varepsilon\to\lambda \text{ weakly}\\ \text{in } W^{\alpha,r}(\Omega;\mathbb{R}^L)}} \mathfrak{G}(t,\lambda^\varepsilon) \ge \mathfrak{G}(t,\lambda) \qquad (53)$$

due to the weak lower-semicontinuity of $\mathfrak{G}(t,\cdot)$.

Let $(u^*,\nu^*) \in Q(\lambda)$ realize the minimum in (21), in particular, $\lambda = \mathcal{L}\bullet\nu^*$. Let further $\lambda_h \to \lambda$ in $W^{\alpha,r}(\Omega;\mathbb{R}^L)$, $\lambda_h \in \Lambda_h$ and let $t_h \to t$ for $h \to 0$. In particular, we again have $\lambda_h \to \lambda$ weakly* in $L^\infty(\Omega;\mathbb{R}^L)$. There is a sequence $\{u_h\}_{h>0} \subset W^{1,p}(\Omega;\mathbb{R}^d)$, u_h piecewise affine on $\mathcal{T}_h$, $\delta_{\nabla u_h} \to \nu^*$ weakly*, where $[\delta_{\nabla u_h}]_x := \delta_{\nabla u_h(x)}$ for $x \in \Omega$, the last δ denoting the Dirac measure. This can be proved by combining the celebrated results by Kinderlehrer and Pedregal [22] with classical approximation results for $W^{1,p}$-functions by element-wise affine functions. Here one uses assumed regularity of the triangulations. Similarly, as in (51) we get

$$\begin{aligned}
\lim_{h\to 0} \int_\Omega \psi(\cdot,\cdot,\theta(t_h)) \bullet \nu_h \mathrm{d}x + \rho|\lambda_h|^r_{W^{\alpha,r}(\Omega;\mathbb{R}^L)} + \frac{1}{\varepsilon}\big\|\lambda_h - \mathcal{L}\bullet\nu_h\big\|^2_{H^{-1}(\Omega;\mathbb{R}^L)} \\
+\frac{1}{2}\int_\Gamma \big(u_h(x) - u_{\mathrm{D}}(t_h,x)\big)^\top A(x)\big(u_h(x) - u_{\mathrm{D}}(t_h,x)\big)\mathrm{d}S \\
= \int_\Omega \psi(\cdot,\cdot,\theta(t)) \bullet \nu \mathrm{d}x + \rho|\lambda|^r_{W^{\alpha,r}(\Omega;\mathbb{R}^L)} \\
+\frac{1}{2}\int_\Gamma \big(u^*(x) - u_{\mathrm{D}}(t,x)\big)^\top A(x)\big(u^*(x) - u_{\mathrm{D}}(t,x)\big)\mathrm{d}S = \mathfrak{G}(t,\lambda). \qquad (54)
\end{aligned}$$

Here we use the L^∞-weak* continuity of the functional $(\lambda,\nu)\mapsto\frac{1}{\varepsilon}\|\lambda-\mathcal{L}\bullet\nu\|^2_{H^{-1}(\Omega;\mathbb{R}^L)}$. This shows that

$$\limsup_{\substack{\lambda_h\to\lambda \text{ in } W^{\alpha,r}(\Omega;\mathbb{R}^L)\\ \lambda_h\in\Lambda_h,\quad t_h\to t,\quad h\to 0}} \mathfrak{G}^\varepsilon_h(t_h,\lambda_h)\le\mathfrak{G}(t,\lambda)\ . \tag{55}$$

Let $(u^\varepsilon,\nu^\varepsilon)$ be a point realizing the infimum in (50). Such $(u^\varepsilon,\nu^\varepsilon)$ exists by coercivity and (weak$\times$weak*)-lower semicontinuity of the functional in (50). As this functional is always majorized by G and coincides with G if (u,ν,λ) is such that $(u,\nu)\in Q(\lambda)$, we have $\mathfrak{G}^\varepsilon(t,\lambda)\le\mathfrak{G}(t,\lambda)$. Consequently we have

$$\lim_{\varepsilon\to 0}\mathfrak{G}^\varepsilon(t,\lambda)\le\mathfrak{G}(t,\lambda). \tag{56}$$

The limit for $\varepsilon\to 0$ indeed exists because $\{\mathfrak{G}^\varepsilon(t,\lambda)\}_{\varepsilon>0}$ is nondecreasing. Therefore, taking (u,ν) minimizing $G(t,\cdot,\cdot,\lambda)$ over $Q(\lambda)$, we have

$$G(t,u^\varepsilon,\nu^\varepsilon,\lambda)\le G(t,u,\nu,\lambda)\ . \tag{57}$$

Thus $(u^\varepsilon,\nu^\varepsilon)$ is bounded in $W^{1,p}(\Omega;\mathbb{R}^d)\times L^\infty_{\rm w}(\Omega;{\rm rca}(\mathbb{R}^{d\times d}))$ and we can extract a subsequence (not relabeled) such that $u^\varepsilon\to w$ weakly and $\nu^\varepsilon\to\sigma$ weakly*. Further we have

$$\lim_{\varepsilon\to 0}\|\lambda-\mathcal{L}\bullet\nu^\varepsilon\|^2_{H^{-1}(\Omega;\mathbb{R}^L)}=\lim_{\varepsilon\to 0}\varepsilon(\mathfrak{G}^\varepsilon(t,\lambda)-V(t,u^\varepsilon,\nu^\varepsilon,\lambda))=0, \tag{58}$$

which at the same time means that $\|\lambda-\mathcal{L}\bullet\sigma\|_{H^{-1}(\Omega;\mathbb{R}^L)}=0$. Therefore, $(w,\sigma)\in Q(\lambda)$ and $G(t,w,\sigma,\lambda)\ge\mathfrak{G}(t,\lambda)$. On the other hand, the limit passage in (57) for $\varepsilon\to 0$ gives $G(t,w,\sigma,\lambda)\le\mathfrak{G}(t,\lambda)$. Altogether it yields

$$\lim_{\varepsilon\to 0}\mathfrak{G}^\varepsilon(t,\lambda)=\mathfrak{G}(t,\lambda). \tag{59}$$

□

Moreover, let us define the *stable set* for the continuous and the discrete problems at time t respectively as

$$S(t)\ :=\big\{\lambda\in\Lambda;\quad\forall\tilde\lambda\in\Lambda\ :\quad\mathfrak{G}(t,\lambda)\ \le\ \mathfrak{G}(t,\tilde\lambda)+\mathfrak{R}(\tilde\lambda-\lambda)\big\}, \tag{60}$$

$$S^\varepsilon_h(t):=\big\{\lambda\in\Lambda_h;\quad\forall\tilde\lambda\in\Lambda_h:\quad\mathfrak{G}^\varepsilon_h(t,\lambda)\le\mathfrak{G}^\varepsilon_h(t,\tilde\lambda)+\mathfrak{R}(\tilde\lambda-\lambda)\big\}. \tag{61}$$

Denoting by "Limsup" the Kuratowski's limit, the following assertion can be interpreted, in other words, as ${\rm Limsup}_{\varepsilon\to 0}{\rm Limsup}_{h\to 0}{\rm Graph}(S^\varepsilon_h)\subset{\rm Graph}(S)$:

Lemma 4.4 *Let (31), (45), (47) hold. If $\lambda^\varepsilon_h\in S^\varepsilon_h(t_h)$, $t_h\to t$ and $\lim_{\varepsilon\to 0}\lim_{h\to 0}\lambda^\varepsilon_h=\lambda$ weakly in $W^{\alpha,r}(\Omega;\mathbb{R}^L)$, then $\lambda\in S(t)$. Moreover,*

$$\lim_{\varepsilon\to 0}\lim_{h\to 0}\mathfrak{G}^\varepsilon_h(t_h,\lambda^\varepsilon_h)=\mathfrak{G}(t,\lambda). \tag{62}$$

Proof. Take $\tilde\lambda \in \Lambda$ arbitrary and, by (46), a sequence $\tilde\lambda_h \in \Lambda_h$ approaching to $\tilde\lambda_h$ in $W^{\alpha,r}(\Omega;\mathbb{R}^L)$. As $\{\tilde\lambda_h\}_{h>0}$ is bounded, we have also $\tilde\lambda_h \to \tilde\lambda$ weakly* in $L^\infty(\Omega;\mathbb{R}^L)$. Then, considering $\lambda_h^\varepsilon \in S_h^\varepsilon(t_h)$ such that $\lambda_h^\varepsilon \to \lambda$ weakly in $W^{\alpha,r}(\Omega;\mathbb{R}^L)$, $t_h \to t$, by (48), we have

$$\begin{aligned}\mathfrak{G}(t,\lambda) &\le \liminf_{\varepsilon\to0}\liminf_{h\to0}\mathfrak{G}_h^\varepsilon(t_h,\lambda_h^\varepsilon) \le \liminf_{\varepsilon\to0}\liminf_{h\to0}\mathfrak{G}_h^\varepsilon(t_h,\tilde\lambda_h)+\mathfrak{R}(\lambda_h-\tilde\lambda_h) \\ &\le \lim_{\varepsilon\to0}\limsup_{h\to0}\mathfrak{G}_h^\varepsilon(t_h,\tilde\lambda_h)+\lim_{h\to0}\mathfrak{R}(\lambda_h-\tilde\lambda_h) \le \mathfrak{G}(t,\tilde\lambda)+\mathfrak{R}(\lambda-\tilde\lambda).\end{aligned} \tag{63}$$

We used the weak* continuity of $\mathfrak{R}: W^{\alpha,r}(\Omega;\mathbb{R}^L)\to\mathbb{R}$, which is due to the compactness of the embedding $W^{\alpha,r}(\Omega;\mathbb{R}^L)\subset L^1(\Omega;\mathbb{R}^L)$ and the continuity of $\mathfrak{R}: L^1(\Omega;\mathbb{R}^L)\to\mathbb{R}$. In view of (60), it just says that $\lambda\in S(t)$. Moreover, putting $\tilde\lambda:=\lambda$ into (63) yields (62). □

Further we will use the following "nonbuckling" condition; as already remarked, a finer technique [14] allows to avoid this not much realistic condition. Anyhow, for (u,ν) a point realizing the infimum in (27) with a given pair (t,λ), the "nonbuckling" condition says that

$$\begin{aligned}&t_h\to t \quad\&\quad \lambda_h\to\lambda \text{ weakly* in } W^{\alpha,r}(\Omega;\mathbb{R}^L) \quad\&\quad h\to0 \quad\&\quad \lambda_h\in\Lambda_h\\ &\Rightarrow\quad u_h\to u \text{ weakly in } W^{1,p}(\Omega;\mathbb{R}^d) \;\&\; \nu_h\to\nu \text{ weakly* in } L^\infty_{\rm w}(\Omega;{\rm rca}(\mathbb{R}^{d\times d})).\end{aligned} \tag{64}$$

Similar condition has also been used in [30].

Lemma 4.5 *If $\theta\in C^1([0,T])$ and the "nonbuckling" condition (64) holds then*

$$\lim_{\substack{\varepsilon\to0,\quad \lambda_h\in\Lambda_h,\quad t_h\to t,\quad h\to0\\ \lambda_h\to\lambda \text{ weakly in } W^{\alpha,r}(\Omega;\mathbb{R}^L)}} \frac{\partial\mathfrak{G}_h^\varepsilon}{\partial t}\big(t_h,\lambda_h\big)=\frac{\partial\mathfrak{G}}{\partial t}\big(t,\lambda\big) \tag{65}$$

for all $(t,\lambda)\in[0,T]\times\Lambda$.

Proof. As to (65), we realize that

$$\begin{aligned}\frac{\partial\mathfrak{G}_h^\varepsilon}{\partial t}\big(t_h,\lambda_h\big) &= \int_\Gamma A(x)(u_h(x)-u_{\rm D}(t_h,x))\frac{\partial u_{\rm D}}{\partial t}(t_h,x){\rm d}S\\ &+ \int_\Omega\Big(\frac{\partial\psi}{\partial\theta}(\cdot,\theta(t_h))\bullet\nu_h\Big)\frac{{\rm d}\theta}{{\rm d}t}(t_h){\rm d}x\end{aligned} \tag{66}$$

where (u_h,ν_h) is the minimizer in the optimization problem involved in (27) with $(t,\lambda):=(t_h,\lambda_h)$. Due to (64), we may suppose that $u_h\to u$ weakly in $W^{1,p}(\Omega;\mathbb{R}^d)$ and $\nu_h\to\nu$ weakly* in $L^\infty_{\rm w}(\Omega;{\rm rca}(\mathbb{R}^{d\times d}))$. Then also $u_h|_\Gamma\to u|_\Gamma$ strongly in $L^2(\Gamma;\mathbb{R}^d)$. Moreover, by the dominated-convergence theorem, we also have $\frac{\partial u_{\rm D}}{\partial t}(t_h,\cdot)\to\frac{\partial u_{\rm D}}{\partial t}(t,\cdot)$ strongly in $L^2(\Gamma;\mathbb{R}^d)$. As $A\in L^\infty(\Omega;\mathbb{R}^{d\times d})$ and $u_{\rm D}(t_h,\cdot)\to u_{\rm D}(t,\cdot)$ strongly in $L^2(\Gamma;\mathbb{R}^d)$ we get the convergence of the first term on the right-hand side in (66) to

$\int_\Gamma A(x)(u(x)-u_{\rm D}(t,x))\frac{\partial u_{\rm D}}{\partial t}(t,x){\rm d}S$. Further notice that $\partial\hat\psi/\partial\theta(F,\cdot)$ with $\hat\psi$ from (3) is continuous for positive arguments θ. Thus, if $\theta\in C^1(I)$ is positive, we get the convergence of the second term in the right-hand side of (66) to $\int_\Omega(\frac{\partial\psi}{\partial\theta}(\cdot,\theta(t))\bullet\nu_h)\frac{{\rm d}\theta}{{\rm d}t}(t){\rm d}x$. □

Using the above results we can prove the convergence:

Proposition 4.6 *Let the assumptions (31), (32), (45), (47) (64) be valid, and $\theta\in C^1([0,T])$. Then there is a subsequence $\{\lambda^\varepsilon_{\tau,h}\}_{\tau>0,h>0}$, denoted for simplicity by the same index (τ,h), and a limit process $\lambda:[0,T]\to\Lambda$ such that:*

(i) $\lim_{\varepsilon\to0}\lim_{\tau\to0,h\to0}\lambda^\varepsilon_{\tau,h}(t)=\lambda(t)$, *i.e. weak convergence in $L^1(\Omega;\mathbb{R}^L)$ for all $t\in[0,T]$, and $\lambda\in L^\infty([0,T]\times\Omega;\mathbb{R}^L)\cap{\rm BV}([0,T];L^1(\Omega;\mathbb{R}^L))$,*

(ii) $\lim_{\varepsilon\to0}\lim_{\tau\to0,h\to0}\mathfrak{G}^\varepsilon_{\tau,h}(t,\lambda^\varepsilon_{\tau,h}(t))=\mathfrak{G}(t,\lambda(t))$ *for all $t\in[0,T]$.*

Moreover, every such limit process λ is a solution process in the sense that $\lambda(t)$ is stable in the sense of (24a) and the energy inequality (24b) holds even as an equality for every s and t with $0\le s<t\le T$.

Proof. For clarity, let us divide it into three steps.

Step 1: The points (i)–(ii). By the a-priori estimate (36) and Helly's selection principle (see Barbu and Precupanu [7]), we can select the subsequence and a function $\mathcal{G}\in{\rm BV}([0,T])$ such that $\lim_{\varepsilon\to0}\lim_{\tau\to0,h\to0}\mathfrak{G}^\varepsilon_{\tau,h}(t,\lambda^\varepsilon_{\tau,h}(t))=\mathcal{G}(t)$ for all $t\in[0,T]$. Furthermore, taking into account the a-priori estimate (35), by a generalized Helly selection principle for Banach-space valued functions, see [32, Theorem 6.1], we can make the selection in such a way that, for some $\lambda\in{\rm BV}(0,T;L^1(\Omega;\mathbb{R}^L))$, $\lambda^\varepsilon_{\tau,h}(t)\to\lambda(t)$ weakly in $L^1(\Omega;\mathbb{R}^L)$ for all $t\in[0,T]$.

By stability (33) and in view of the definition of $\mathfrak{G}^\varepsilon_{\tau,h}$, we can write $\mathfrak{G}^\varepsilon_{\tau,h}(t,\lambda^\varepsilon_{\tau,h}(t))=\mathfrak{G}^\varepsilon_h(\vartheta(t,\tau),\lambda^\varepsilon_{\tau,h}(t))$ for some $\vartheta(t,\tau)\in[t,T]$ such that $\lim_{\tau\to0}\vartheta(t,\tau)=t$; in fact, $\vartheta(t,\tau)$ is $\min_{k\in\mathbb{N}\cup\{0\}}\{k\tau\ge t\}$. As in (62), we now have $\lim_{\varepsilon\to0}\lim_{\tau,h\to0}\mathfrak{G}^\varepsilon_{\tau,h}(t,\lambda^\varepsilon_{\tau,h}(t))=\mathfrak{G}(t,\lambda(t))$. Comparing it with what we got by Helly's selection principle, we can see that $\mathcal{G}(t)=\mathfrak{G}(t,\lambda(t))$ for all $t\in[0,T]$, which proves (ii).

Step 2: $\lambda(t)\in S(t)$ for all t. Let us fix t. As $\lambda^\varepsilon_{\tau,h}(t)\in S^\varepsilon_h(\vartheta(t,\tau))$ with $\vartheta(\cdot,\cdot)$ from Step 1, by using Lemma 4.4, we can see that $\lambda(t)\in S(t)$.

Step 3: The energy (in)equality (24b). First, let us consider $s=0$ and t as some grid-point belonging to some partition of $[0,T]$. Then (34) is at our disposal for each finer partition and for the limit passage, we will therefore consider only those partitions, i.e. with τ small enough with respect to this t. Again, we use $\lim_{\varepsilon\to0}\lim_{\tau\to0}\mathfrak{G}^\varepsilon_{\tau,h}(t,\lambda^\varepsilon_{\tau,h}(t))=\mathfrak{G}(t,\lambda(t))$. From the pointwise converge of $\lambda^\varepsilon_{\tau,h}(\cdot)$ and from the definition (25) of ${\rm Var}_L(\lambda^\varepsilon_{\tau,h};0,t)$, we get $\liminf_{\varepsilon\to0}\liminf_{\tau,h\to0}{\rm Var}_L(\lambda^\varepsilon_{\tau,h};0,t)\ge{\rm Var}_L(\lambda;0,t)$. Moreover, as we proved $\lambda^\varepsilon_{\tau,h}(t)\to\lambda(t)$ weakly in $L^1(\Omega;\mathbb{R}^L)$ and, by (35), this sequence is bounded in $W^{\alpha,r}(\Omega;\mathbb{R}^L)$ and therefore $\lambda^\varepsilon_{\tau,h}(t)\to\lambda(t)$ weakly also in $W^{\alpha,r}(\Omega;\mathbb{R}^L)$. Then, by (65), $\frac{\partial}{\partial t}\mathfrak{G}^\varepsilon_{\tau,h}\big(t,\lambda^\varepsilon_{\tau,h}(t)\big)=\frac{\partial}{\partial t}\mathfrak{G}^\varepsilon_h\big(\vartheta(t,\tau),\lambda^\varepsilon_{\tau,h}(t)\big)\to\frac{\partial}{\partial t}\mathfrak{G}\big(t,\lambda(t)\big)$. Therefore,

$$\int_0^t\frac{\partial\mathfrak{G}^\varepsilon_h}{\partial\vartheta}\big(\vartheta,\lambda^\varepsilon_{\tau,h}(\vartheta)\big){\rm d}\vartheta\to\int_0^t\frac{\partial\mathfrak{G}}{\partial\vartheta}\big(\vartheta,\lambda(\vartheta)\big){\rm d}\vartheta\tag{67}$$

by the Lebesgue dominated-convergence theorem when using the a-priori bounds like in (42). Moreover, $\lambda^\varepsilon_{\tau,h}(\vartheta-\tau)\to\lambda(t)$ weakly in $L^1(\Omega;\mathbb{R}^L)$ provided t is a point of continuity of $\lambda(\cdot)$, i.e. for a.a. $t\in[0,T]$ because BV-functions are a.e. continuous. Due to the a-priori estimate (35), again we also have this convergence weakly in $W^{\alpha,r}(\Omega;\mathbb{R}^L)$. Therefore also

$$\int_0^t \frac{\partial\mathfrak{G}^\varepsilon_h}{\partial\vartheta}\big(\vartheta,\lambda^\varepsilon_{\tau,h}(\vartheta-\tau)\big)\mathrm{d}\vartheta\to\int_0^t\frac{\partial\mathfrak{G}}{\partial\vartheta}\big(\vartheta,\lambda(\vartheta)\big)\mathrm{d}\vartheta. \tag{68}$$

Then, we can pass to the limit in both inequalities in (34), proving thus

$$\mathfrak{m}(\mathfrak{t}):=\mathfrak{G}\big(\mathfrak{t},\lambda(\mathfrak{t})\big)-\mathfrak{G}\big(\mathfrak{o},\lambda_\mathfrak{o}\big)+\mathrm{Var}_\mathfrak{L}(\lambda;\mathfrak{o},\mathfrak{t})+\int_\mathfrak{o}^\mathfrak{t}\frac{\partial\mathfrak{G}}{\partial\vartheta}\big(\vartheta,\lambda(\vartheta)\big)\mathrm{d}\vartheta=\mathfrak{o} \tag{69}$$

at each t of the form $k\tau\in[0,T]$, $k=1,...,T/\tau$, τ from the considered sequence of time steps. The (only countable) set of such t's is dense in $[0,T]$ and thus (69) must hold also at each $t\in[0,T]$ at which all functions involved in (69) are continuous. Those functions have, however, a bounded variations and are thus continuous with the exception of at most countable number of points. Hence (69) holds everywhere on $[0,T]$ with the only exception of at most countable number of points.

Then, a proof of continuity of $\mathfrak{m}$ on $[0,T]$ can be performed as in [30, Step 6 of the proof of Theorem 3.4]. Thus (24b) for general $s\le t$ can be proved. □

5 Computer implementation of the minimization problem (26)

A computer realization of (26) is made for $d=3$ but involves several simplifications. In particular, we do not implement the regularization of V, i.e. we put $\rho=0$ in V, do not implement the penalization scheme and define $\hat\psi:=\min_\ell\hat\psi_\ell$ which keeps the wells precisely at the desired orbits $\mathrm{SO}(3)U_\ell$. We implemented piecewise affine tetrahedral finite elements with a standard division of a prism into five tetrahedra. Thus,

$$u_h\in\mathcal{U}_h=\big\{v\in C(\bar\Omega;\mathbb{R}^3);\ \forall\,E\in\mathcal{T}_h:\ v|_E\text{ is affine}\big\}\ . \tag{70}$$

This means that ∇u_h is element-wise constant, as used for the approximation in Section 4. In view of the specific experiments in Sect. 6, the choice $\kappa=1$, i.e. the first-order laminates described in (6), is chosen so that we can write

$$\begin{aligned}&F_{1h}=\nabla u_h+(1-\xi_h)a_h\otimes n_h\ ,\qquad F_{2h}=\nabla u_h-\xi_h a_h\otimes n_h\ ,\\&\text{where }\xi_h\in L^\infty(\Omega);\quad 0\le\xi_h\le1,\quad\forall\,E\in\mathcal{T}_h:\quad \xi_h|_E\text{ is constant},\\&\qquad a_h,n_h\in L^\infty(\Omega;\mathbb{R}^3);\quad\forall\,E\in\mathcal{T}_h:\quad a_h|_E,\ n_h|_E\text{ are constant.}\end{aligned} \tag{71}$$

Finally, it is clear that

$$[\nu_h]_x=\xi_h(x)\delta_{F_{1h}(x)}+(1-\xi_h(x))\delta_{F_{2h}(x)}\ ,\quad x\in\Omega, \tag{72}$$

represents an element-wise constant first-order laminate. Consequently, any Young measure (72) is fully determined by ∇u_h, ξ_h, a_h and n_h. As to the construction of the dissipation potential, we calculate for a given $F \in R^{d\times d}$ its right Cauchy-Green tensor $C = F^\top F$ and calculate the square of the Euclidean distance of C to all $C_\ell = F_\ell^\top F_\ell$, $\ell = 1, \dots, L$. Taking a smooth function $\tilde{d} : \mathbb{R} \to \mathbb{R}$ such that $\tilde{d} = 1$ in a neighborhood of 0 and $\tilde{d} = \delta$ otherwise for some $\delta > 0$ small, we can see that

$$\left\{ \frac{\tilde{d}(\mathrm{dist}^2(C, C_m))}{\sum_{\ell=1}^{L} \tilde{d}(\mathrm{dist}^2(C, C_\ell))} \right\}_{m=1}^{L} \in \triangle_L \ .$$

This construction defines the mapping $\mathfrak{L} : \mathbb{R}^{d\times d} \to \triangle_L$. The norm on $\mathbb{R}^L$ is taken as $|\lambda|_L = \sum_{i=1}^{L} \gamma_i |\lambda_i|$ where $\gamma_i > 0$ for $1 \le i \le L$.

Moreover, we replace the nonsmooth absolute value by its regularization $|y| \approx \sqrt{y^2 + \beta}$ with $\beta = 10^{-8}$. Defining

$$\Psi(t, u, \nu, \nu^{k-1}) = \int_\Omega \int_{\mathbb{R}^{d\times d}} \hat{\psi}(F, \theta(t)) \nu_x(dF)\, dx + \int_\Omega \left| \mathfrak{L} \bullet \nu - \mathfrak{L} \bullet \nu^{k-1} \right|_L \mathrm{d}x \tag{73}$$

$$+ \frac{1}{2} \int_\Gamma (u(x) - u_{\mathrm{D}}(t, x))^\top A(x)(u(x) - u_{\mathrm{D}}(t, x))\, \mathrm{d}x \tag{74}$$

and setting the initial condition ν_0 we have the following problem for $k = 1, \dots, T/\tau$:

$$\left.\begin{array}{ll} \text{Minimize} & \Psi(k\tau, u, \nu, \nu^{k-1}) \\ \text{subject to} & u \in \mathcal{U}_h \ , \quad \nu \text{ is given by (72).} \end{array}\right\} \tag{75}$$

The problem (75) is solved by the the optimization routine "L-BFGS-B" described in [10]. Due to the multi-well character of $\hat{\psi}$, (75) is a nonconvex minimization problem, which, together with rather big number of variables, makes finding a global minimum extremely difficult. As "L-BFGS-B" is designed for local optimization, we need some strategy to rule out at least some of local minima. Notice that, since we use a first-order laminate, i.e., a two-atomic probability measure, we can relatively easily reach a microstructure consisting of no more than two material phases/variants, while more complicated microstructures can be reached, as we proved in Section 4, rather theoretically only by using very fine discretizations allowing indeed fast spatial oscillations. The idea is to neglect some energy wells by assigning them "infinite" energy and compare obtained values of the minima in (75) for the original $\hat{\psi}$ and modified $\hat{\psi}$ with some wells neglected. Our experience shows that at least in simple experiments this strategy leads to reasonable results.

6 Computational experiments with a NiMnGa single crystal

We performed our computational on a prismatic single crystal of Ni_2MnGa in a specific orientation, mostly (1,0,0). This alloy (or, more precisely, intermetalic) undergoes a

cubic/tetragonal transformation, which is relatively easy to model because the martensite forms only 3 variants.

6.1 The data

The mentioned 3 variants of martensite are described by $U_2 = \mathrm{diag}(\eta_2, \eta_1, \eta_1)$, $U_3 = \mathrm{diag}(\eta_1, \eta_2, \eta_1)$ and $U_4 = \mathrm{diag}(\eta_1, \eta_1, \eta_2)$ where $\eta_1 = 1.018$ and $\eta_2 = 0.9608$. The stretch tensor of the austenite is the identity, i.e. $U_1 = \mathrm{diag}(1, 1, 1)$. Therefore, $L = 4$ in our example. Using [6] we can see that martensitic variants are rank-one connected with each other while none of them is rank-one connected with the austenite. Rank-one connection allows for the formation of a planar interface between two martensitic variants. We prescribe the dissipation energy density as 0.35 MPa for transformations between the austenite and any martensitic variant ([1]) and almost no dissipation is assumed for transformations among martensitic variants. This can be done by taking $\gamma_1 = 35 \times 10^4$ and $\gamma_i = 1$ if $i \neq 1$. The equilibrium temperature of the austenite and martensite is about 288 K (i.e. 35°C), the energetic minimum of the martensites changes with the temperature at the rate 200 kPa/K. Roughly speaking, after dividing this rate by a transformation strain (here about 6%), we get a so-called *Clausius-Clapeyron constant* (here about 3 MPa/K). In view of (2)-(3) with θ_0 considered as 288 K, this constant is essentially the difference of the heat capacity c_1 in austenite from the heat capacity $c_2 = c_3 = c_4$ in the martensite.

Elastic moduli of the austenite are taken zero but $\mathcal{C}^1_{1111} = 13.6$ GPa, $\mathcal{C}^1_{1122} = \mathcal{C}^1_{2211} = 9.2$ GPa, $\mathcal{C}^1_{2323} = \mathcal{C}^1_{2332} = \mathcal{C}^1_{3223} = \mathcal{C}^1_{3232} = 10.2$ GPa. Here we are inspired by an experiment presented in [1] where the measured elastic moduli are artificially taken smaller by a factor 10 to reflect a certain "pre-martensitic transformation" observed experimentally in this particular alloy. Elastic moduli of all martensitic variants are then taken as those measured in austenite, i.e. $\mathcal{C}^\ell_{1111} = 136$ GPa, $\mathcal{C}^\ell_{1122} = \mathcal{C}^\ell_{2211} = 92$ GPa, $\mathcal{C}^\ell_{2323} = \mathcal{C}^\ell_{2332} = \mathcal{C}^\ell_{3223} = \mathcal{C}^\ell_{3232} = 102$ GPa and zero otherwise for $\ell = 2, 3, 4$, which is again a rather coarse simplification due to missing measurements of such constants.

The specimen is a prism, $\Omega = (0, 9) \times (0, 4) \times (0, 4)$ (in mm's), discretized into tetrahedral elements, cf. Fig.1a. The loading of the specimen is realized through the matrix A and u_{D}. For Fig. 1b, on the side $\{0\} \times (0, 4) \times (0, 4)$ we take A and u_{D} simulating either zero Dirichlet boundary conditions on u_1, this means that A is a diagonal matrix with zeros at appropriate positions on the diagonal and $u_{\mathrm{D}} = 0$.

6.2 Stress-induced PT in a (1,0,0)-oriented single crystal

Computations have proved to perform much better if the specimen is loaded by a simple surface force than by a "spring" load defined by A and u_{D} on the side $\{9\} \times (0, 4) \times (0, 4)$. Therefore we applied a normal surface force at the side $\{9\} \times (0, 4) \times (0, 4)$. However, this regime can be seen as a limit case of the "spring" load if $|A| \to 0$ and $|u_{\mathrm{D}}| \to \infty$. Other parts of the boundary Γ are free, i.e., $A(x) = 0$ if $x \neq (0, x_2, x_3)$.

The loading force on the side $\{9\} \times (0,4) \times (0,4)$ is of a sawtooth form with 150 steps per period; note that, as the process is rate-independent, the actual time scale is irrelevant. The Young-measure initial condition is $\nu_0 = \delta_I$ in Figures 1,3 and 4, while the initial condition in Figure 2 is inhomogeneous.

The following figure simulates a simple lab experiment in a pseudo-elastic regime. The temperature is about 50 °C. This calculation serves as a fitting experiment to our model, by considering experimental data from [1]. Also, in view of both experimental and computational experience in [1], we rely on that the first-order laminate will well suffice for efficient simulation in this particular experiment, which is why $\kappa = 1$ is chosen, cf. (71)-(72).

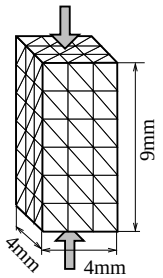

Fig. 1a Geometry of a specimen, two loaded sides, and a triangulation.

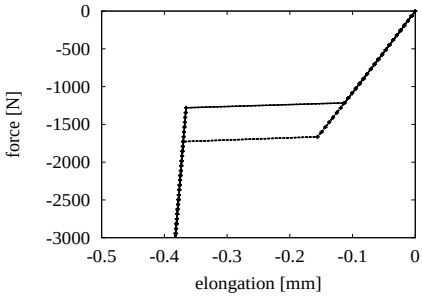

Fig. 1b Loading/compression curve of a Ni_2MnGa single crystal at $\theta = 50°\,C$.

6.3 Temperature-induced PT in a (1,0,0)-oriented single crystal

For the further calculations, A is a diagonal matrix with large positive entries and again $u_{\mathrm{D}} = 0$ simulating zero Dirichlet boundary conditions on all components of u. The second figure shows a typical hysteretic behavior of the strain if the specimen is cyclically heated up and cooled down.

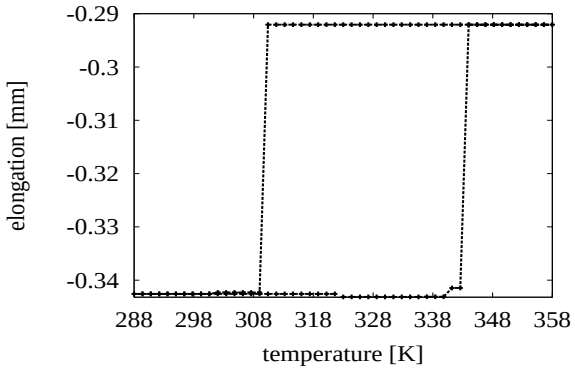

Fig. 2 The specimen under the load of -200 MPa is heated up and then cooled down. A hysteretic response of the temperature vs. elongation.

6.4 Influence of boundary conditions on stress-induced PT

Further, we will demonstrate the influence of the boundary conditions, and in particular we want to obtain a stress/strain response (cf. Fig. 4 below) closer to typical experimental outlet. We load the specimen at all directions on the side $\{0\} \times (0,4) \times (0,4)$, and we can see on Fig. 3 that the specimen does not transform from the austenite to the martensite close to the mentioned piece of the boundary.

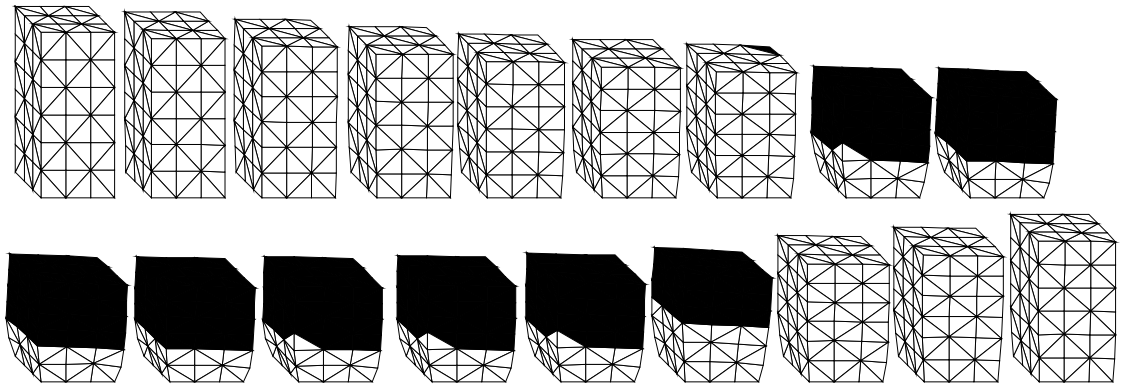

Fig. 3 Spatial evolution of the martensite (black) in the specimen during the compression loading cycle. The displacement is displayed as $10\times$ *magnified.*

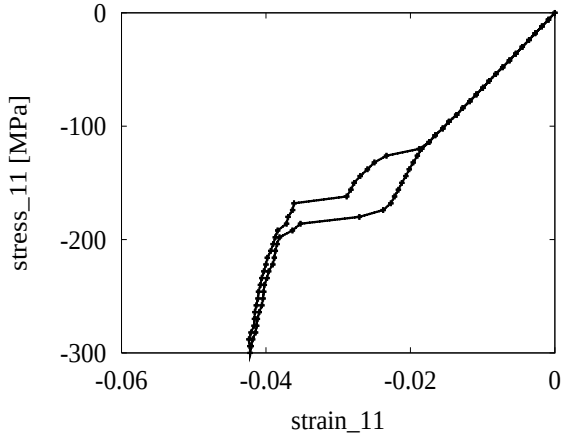

Fig. 4 Pseudo-elastic stress-strain response under the compression test during the loading cycle from Fig. 3.

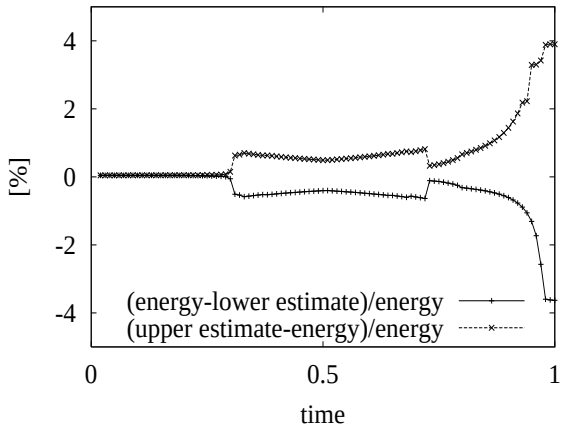

Fig. 5 Energy balance calculated using (34) for the loading cycle from Fig. 3.

Our next figure simulates a reorientation of the martensite. We start from an almost stress-free mixture of martensitic variants with the spatially homogeneous macroscopic deformation gradient $\mathrm{diag}(0.998, 0.998, \eta_1)$. We prescribe $[u_{\mathrm{D}}]_2(x) = 0.002x_1$, $[u_{\mathrm{D}}]_3(x) = (\eta_1 - 1)x_3$ if $x \in \{0\} \times (0,4) \times (0,4) \cup \{9\} \times (0,4) \times (0,4)$, $[u_{\mathrm{D}}]_1 = 0$ on $\{0\} \times (0,4) \times (0,4)$ and $[u_{\mathrm{D}}]_1$ changes in time on $\{9\} \times (0,4) \times (0,4)$ giving the strain $\pm 5\%$. The initial condition is $\nu_0 = \frac{1}{2}\delta_{U_2} + \frac{1}{2}\delta_{U_3}$. Note that calculated Young measures consist, in general,

of two atoms, i.e. a nontrivial spatially inhomogeneous first-order laminate occurs during the most periods of this experiment.

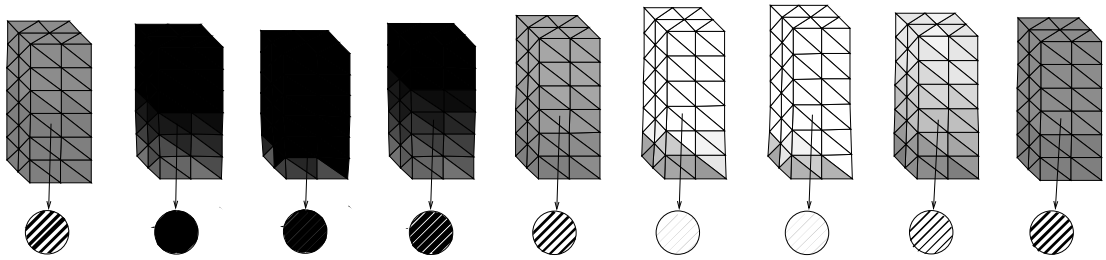

Fig. 6 Evolution of a martensitic reorientation during quasi-plastic cycling at $\theta = 20°C$ showing martensitic variants U_2 (black) and U_3 (white) in the specimen during the loading cycle. Evolving microstructure with the normal of laminates $(1, 1, 0)$ is depicted on one element. The displacement is displayed as magnified by the factor 2. The specimen is here discretized into 120 elements.

Our next experiment shows the reorientation of the martensite during the loading of the specimen by a body force in the horizontal direction. This allows for contemporaneous increase in volume fractions of the martensitic variants U_2 and U_3 in different regions of the specimen.

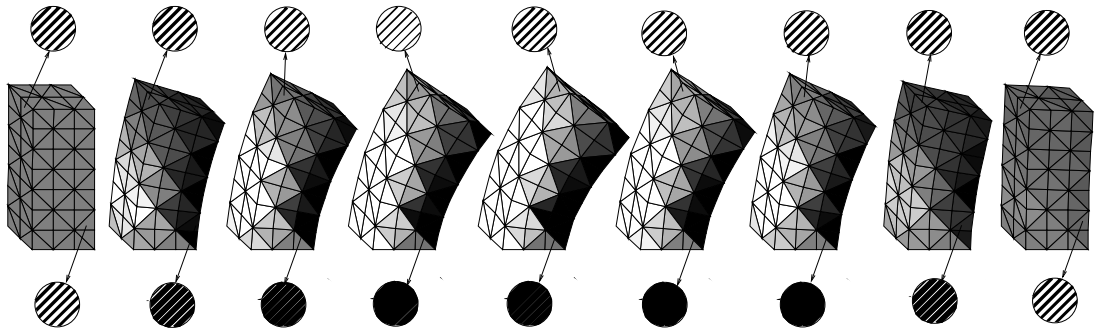

Fig. 7 Evolution of a martensitic reorientation at $\theta = 20°C$ showing martensitic variants U_2 (black) and U_3 (white) in the specimen during the loading by a body force in the horizontal direction. The displacement is displayed as magnified by the factor 3. Again, a laminated microstructure is shown at particular elements.

6.5 Influence of orientation on stress-induced PT

Our last two experiments are very similar to the one depicted in Figure 3, only the orientation of the crystal is different. The crystal lattice is rotated 5 (Fig. 8,9-right) and 2.5 degrees (Fig. 9-midlle) in the plane x_1x_2, i.e., in the plane of the paper, with respect

to the global coordinate system. As the displacement is 5 times magnified the rotational distortion of the specimen is clearly visible.

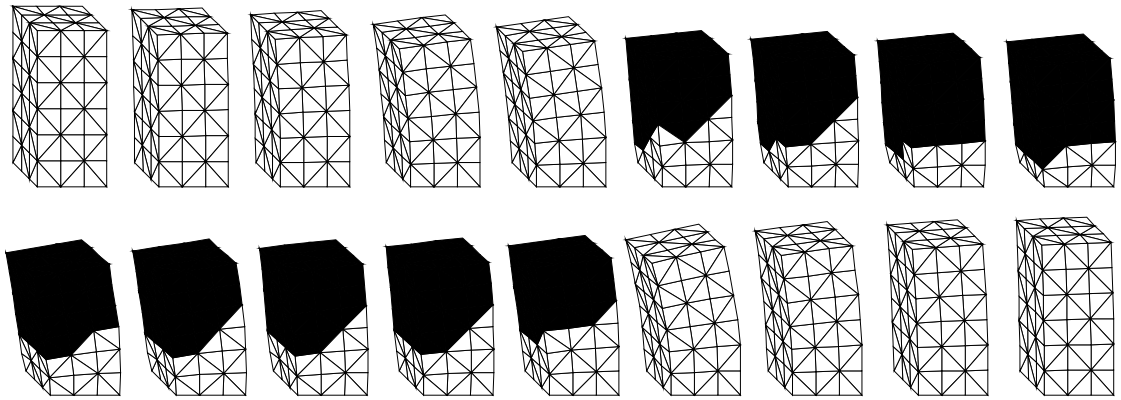

Fig. 8 Spatial evolution of the martensite (black) in the specimen during the compression loading cycle as on Fig. 3 but here with a single crystal in a (1,tg(5°),0)-orientation; the displacement is displayed as 5× magnified.

Our last figure shows stress-strain response calculated in the experiment from Fig. 8, compared both with the basic orientation (1,0,0) as already displayed on Figure 4 and also with an smaller rotation by 2.5 degrees.

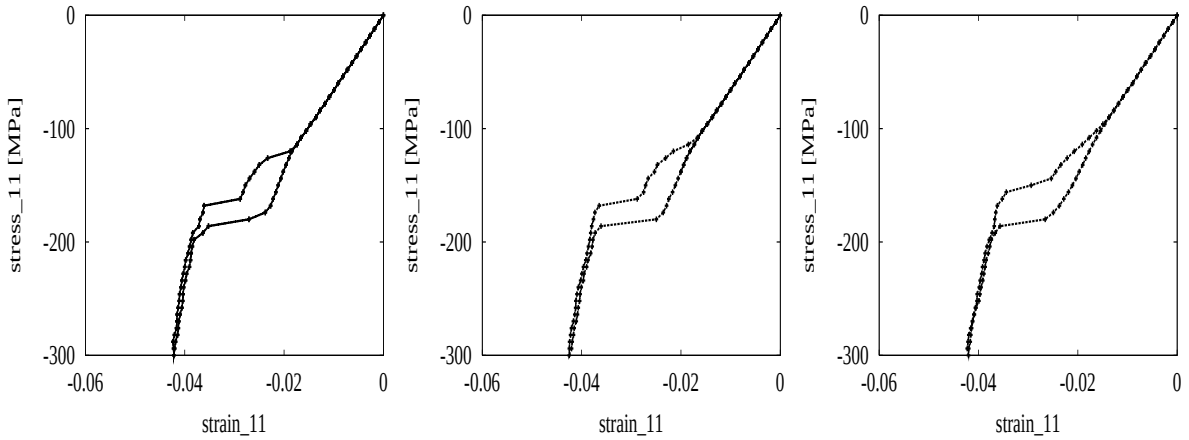

Fig. 9 Comparison of the pseudo-elastic stress-strain response under the compression test for different orientation of the single crystal: left (1,0,0)-oriented, middle rotated by 2.5°, right rotated by 5°.

All the computations are fairly robust in the sense that the curves of material response do not significantly change if we use a finer spatial discretization.

Acknowledgments. The authors are thankful for stimulating discussions during a long term collaboration to A. Mielke, V. Novák, and P. Šittner. This research of M.K. has been partly covered by the grant IAA 1075402 (GA AV ČR) while T.R. has been partly supported by the grants 201/03/0934 (GA ČR), and MSM 11320007 (MŠMT ČR).

References

[1] Arndt, M., Griebel, M., Novák, V., Roubíček, T., Šittner, P.: Martensitic/austenitic transformation in NiMnGa: simulation and experimental approaches. In preparation.

[2] Arndt, M., Griebel, M., Roubíček, T.: Modelling and numerical simulation of martensitic transformation in shape memory alloys. *Continuum Mech. Thermodyn.* **15** (2003), 463-485.

[3] Aubri, S., Fago, M., Ortiz, M.: A constrained sequential-lamination algorithm for the simulation of sub-grid microstructure in martensitic materials. *Comp. Meth. in Appl. Mech. Engr.* 192 (2003), 2823–2843.

[4] Ball, J.M., Holmes, P.J., James, R.D., Pego, R.L., Swart P.J.: On the dynamics of fine structure. *J. Nonlinear Science* **1** (1991), 17–70.

[5] Ball, J.M., James, R.D.: Fine phase mixtures as minimizers of energy. *Archive Rat. Mech. Anal.* **100** (1988), 13–52.

[6] Ball, J.M., James, R.D.: Proposed experimental tests of a theory of fine microstructure and the two-well problem. *Phil. Trans. Royal Soc. London* A **338** (1992), 389–450.

[7] Barbu, V., Precupanu, T.: *Convexity and Optimization in Banach spaces.* D. Reidel Publ.; Dordrecht, 2nd ed.; 1986.

[8] Bhattacharya, K.: *Microstructure of martensite. Why it forms and how it gives rise to the shape-memory effect.* Oxford Univ. Press, 2003.

[9] Brokate, M. Sprekels, J.: *Hystreresis and Phase Transitions.* Springer, New York, 1996.

[10] Byrd, R.H., Lu, P., Nocedal, J., Zhu, C. A limited memory algorithm for bound constrained optimization, *SIAM J. Scientific Computing* **16** (1995), 1190–1208.

[11] Carstensen, C., Plecháč, P.: Numerical analysis of a relaxed variational model of hysteresis in two-phase solids. *Math. Model. Numer. Anal.* **35** (2001), 865–878.

[12] Colli, P.: Global existence for the three-dimensional Frémond model of shape memory alloys. *Nonlinear Analysis, T.M.A.* **24** (1995), 1565-1579.

[13] Colli, P., Frémond, M. and Visintin, A.: Thermo-mechanical evolution of shape memory alloys. *Quarterly Appl. Math.* **48** (1990), 31–47.

[14] Frankfort, G., Mielke, A. An existence result for a rate-independent material model in the case of nonconvex elastic energies. In preparation.

[15] Frémond, M.: *Non-Smooth Thermomechanics.* Springer, Berlin, 2002.

[16] Govindjee, S., Miehe, Ch.: A multi-variant martensitic phase transformation model: formulation and numerical implementation. *Comp. Meth. in Appl. Mech. Engr.* **191** (2001), 215–238.

[17] Hall, G.J., Govindjee, S.: Application of a partially relaxed shape memory free energy function to estimate the phase diagrm and predict global microstructure evolution. *J. Mech. Phys. Solids* **50** (2002), 501–530.

[18] Hill, R.: A variational principle of maximum plastic work in classical plasticity. *Q. J. Mech. Appl. Math.* **1** (1948), 18–28.

[19] Hoffmann, K.-H., Zochowski, A.: Analysis of the thermoelastic model of a plate with non-linear shape-memory alloy reinforcement. *Math. Methods in the Applied Sciences* **15** (1992), 631–645.

[20] Huo, Y., Müller, I.: Nonequilibrium thermodynamics of pseudoelasticity. *Continuum Mech. Thermodyn.* **5** (1993), 163–204.

[21] James, R.D., Hane, K.F.: Martensitic transformations and shape-memory materials. *Acta Mater.* **48** (2000), 197–222.

[22] Kinderlehrer, D., Pedregal, P.: Gradient Young measures generated by sequences in Sobolev spaces. *J. Geom. Anal.* **4** (1994), 59–90.

[23] Kružík, M.: Numerical approach to double-well problem. *SIAM J. Numer. Anal.* **35** (1998), 1833-1849.

[24] Kružík, M., Luskin, M.: The computation of martensitic microstructure with piecewise laminates. *J. Sci. Comp.* **19** (2003), 293–308.

[25] Levitas, V.I.: Thermomechanical theory of martensitic phase transformations in inelastic material. *Int. J. Solids Structures* **35** (1998), 889–940.

[26] Luskin, M.: Approximation of a laminated microstructure for a rotationally invariant, double well energy density. *Numer. Math.* **75** (1996), 205–221.

[27] Luskin, M.: Numerical analysis of a microstructure for a rotationally invariant, double well energy. *Z. Angew. Math. Mech.* **76** Suppl. 2 (1996), 405–408.

[28] Luskin, M.: On the computation of crystalline microstructure. *Acta Numerica* **5** (1996), 191–257.

[29] Mielke, A.: Analysis of energetic models for rate-independent materials. In: *Int. Congress of Math. 2002*, Beijing, Voll.III, pp.817–828.

[30] Mielke, A., Roubíček, T.: Rate-independent model of inelastic behaviour of shape-memory alloys. *Multiscale Modeling Simul.* **1** (2003), 571-597.

[31] Mielke, A., Theil, F.: A mathematical model for rate-independent phase transformations with hysteresis. In: *Models of continuum mechanics in analysis and engineering.* (Eds.: H.-D.Alder, R.Balean, R.Farwig), Shaker Verlag, Aachen, 1999, pp.117-129.

[32] Mielke, A., Theil, F.: On rate-independent hysteresis models. *Nonlin. Diff. Eq. Appl.* **11** (2004), 151-189.

[33] Mielke, A., Theil, F., Levitas, V.I.: A variational formulation of rate-independent phase transformations using an extremum principle. *Archive Rat. Mech. Anal.* **162** (2002), 137–177.

[34] Müller, I., Seelecke, S.: Thermodynamic aspects of shape memory alloys. *Math. Comp. Modelling* **34** (2001), 1307–1355.

[35] Müller, I., Wilmański, K. A model for phase transitions in pseudoelastic bodies. *Il Nuovo Cimento* **57B** (1980), 283-318.

[36] Müller, S.: Variational models for microstructure and phase transitions. (Lect.Notes No.2, Max-Planck-Institut für Math., Leipzig, 1998). In: *Calculus of variations and geometric evolution problems.* (Eds.: S.Hildebrandt et al.) Lect. Notes in Math. **1713** (1999), Springer, Berlin, pp.85–210.

[37] Nicolaides, R.A., Walkington, N.J.: Computation of microstructure utilizing Young measure representations. In: *Recent Advances in Adaptive and Sensory Materials and their Applications.* (C.A.Rogers, R.A.Rogers, eds.) Technomic Publ., Lancaster, 1992, pp.131–141.

[38] Niezgódka, M., Sprekels, J.: Existence of solutions for a mathematical model of structural phase transitions in shape memory alloys. *Math. Methods in Appl. Sci.* **10** (1988), 197–223.

[39] Pedregal, P.: *Parametrized Measures and Variational Principles.* Birkäuser, Basel, 1997.

[40] Petryk, H., Stupkiewicz, S.: Multi-scale micromechanical modeling of stress-induced martensitic transformation. In: Proc. NATO Workshop *New Trends in Phase Transformations and Their Applications to Smart Structures* (Metz, April 2002), to appear.

[41] Pitteri, M., Zanzotto, G.: *Continuum Models for Phase Transitions and Twinning in Crystals.* Chapman & Hall, Boca Raton, 2003.

[42] Rajagopal, K.R., Srinivasa, A.R.: Mechanics of inelastic behavior of materials. Part I and II. *Int. J. Plasticity* **14** (1998), 945–968,969–998.

[43] Ren, X., Truskinovsky, L.: Finite scale microstructures in nonlocal elasticity. *J. Elasticity* **59** (2000), 319–355.

[44] Rogers, R., Truskinovsky, L.: Discretization and hysteresis. *Physica B* **233** (1997), 370–375.

[45] Roubíček, T.: Dissipative evolution of microstructure in shape memory alloys. In: *Lectures on Applied Mathematics.* (H.-J. Bungartz, R. H. W. Hoppe, C. Zenger, eds.) Springer, Berlin, 2000, pp.45–63.

[46] Roubíček, T.: Evolution model for martensitic phase transformation in shape-memory alloys. *Interfaces and Free Boundaries* **4** (2002), 111-136.

[47] Roubíček, T.: Models of microstructure evolution in shape memory materials. In: NATO Workshop *Nonlinear Homogenization and its Appl. to Composites, Polycrystals and Smart Mater.* (Eds. P. Ponte Castañeda et al.), Kluwer, 2004, pp. 269–304.

[48] Srinivasa, A.R., Rajagopal, K.R., Armstrong, R.W.: A phenomenological model of twinning based on dual reference structures. *Acta Materialia* **46** (1998), 1235–1248.

[49] Šverák, V.: Rank-one convexity does not imply quasiconvexity. *Proc. R. Soc. Edinb.* **120 A** (1992), 185-189.

[50] Thamburaja, P., Anand, L.: Thermomechanically coupled superelastic response of initially-textured TiNi sheet. *Acta Mater.* **51** (2003), 325–338.

[51] Vivet, A., Lexcelent, C.: Micromechanical modelling for tension-compression pseudoelastic behaviour of AuCd single crystals. *Euro Phys.J. A.P.***4**(1998), 125-132.

[52] Wineman, A.S., Rajagopal, K.R.: On a constitutive theory for materials undergoing microstructural changes. *Arch. Mech.* **42** (1990), 53–75.

[53] Young, L.C.: Generalized curves and the existence of an attained absolute minimum in the calculus of variations. *Comptes Rendus de la Société des Sciences et des Lettres de Varsovie*, Classe III **30** (1937), 212–234.